



Unravelling the anticancer potency of 1,2,4-triazole-*N*-arylamide hybrids through inhibition of STAT3: synthesis and in silico mechanistic studies

Abdallah Turkey¹ · Ashraf H. Bayoumi¹ · Farag F. Sherbiny^{1,2} · Khaled El-Adl^{3,4} · Hamada S. Abulkhair^{1,5}

Received: 6 July 2020 / Accepted: 6 August 2020
© Springer Nature Switzerland AG 2020

Abstract

The discovery of potent STAT3 inhibitors has gained noteworthy impetus in the last decade. In line with this trend, considering the proven biological importance of 1,2,4-triazoles, herein, we are reporting the design, synthesis, pharmacokinetic profiles, and in vitro anticancer activity of novel C3-linked 1,2,4-triazole-*N*-arylamide hybrids and their in silico proposed mechanism of action via inhibition of STAT3. The 1,2,4-triazole scaffold was selected as a privilege ring system that is embedded in core structures of a variety of anticancer drugs which are either in clinical use or still under clinical trials. The designed 1,2,4-triazole derivatives were synthesized by linking the triazole-thione moiety through amide hydrophilic linkers with diverse lipophilic fragments. In silico study to predict cytotoxicity of the new hybrids against different kinds of human cancer cell lines as well as the non-tumor cells was conducted. The multidrug-resistant human breast adenocarcinoma cells (MDA-MB-231) was found most susceptible to the cytotoxic effect of synthesized compounds and hence were selected to evaluate the in vitro anticancer activity. Four of the designed derivatives showed promising cytotoxicity effects against selected cancer cells, among which compound **12** showed the highest potency ($IC_{50} = 3.61 \mu\text{M}$), followed by **21** which displayed IC_{50} value of $3.93 \mu\text{M}$. Also, compounds **14** and **23** revealed equipotent activity with the reference cytotoxic agent doxorubicin. To reinforce these observations, the obtained data of in vitro cytotoxicity have been validated in terms of ligand–protein interaction and new compounds were analyzed for ADMET properties to evaluate their potential to build up as good drug candidates. This study led us to identify two novel C3-linked 1,2,4-triazole-*N*-arylamide hybrids of interesting antiproliferative potentials as probable lead inhibitors of STAT3 with promising pharmacokinetic profiles.

Electronic supplementary material The online version of this article (<https://doi.org/10.1007/s11030-020-10131-0>) contains supplementary material, which is available to authorized users.

✉ Hamada S. Abulkhair
hamadaorganic@azhar.edu.eg; habulkhair@horus.edu.eg

¹ Pharmaceutical Organic Chemistry Department, Faculty of Pharmacy, Al-Azhar University, Nasr City, Cairo 11884, Egypt

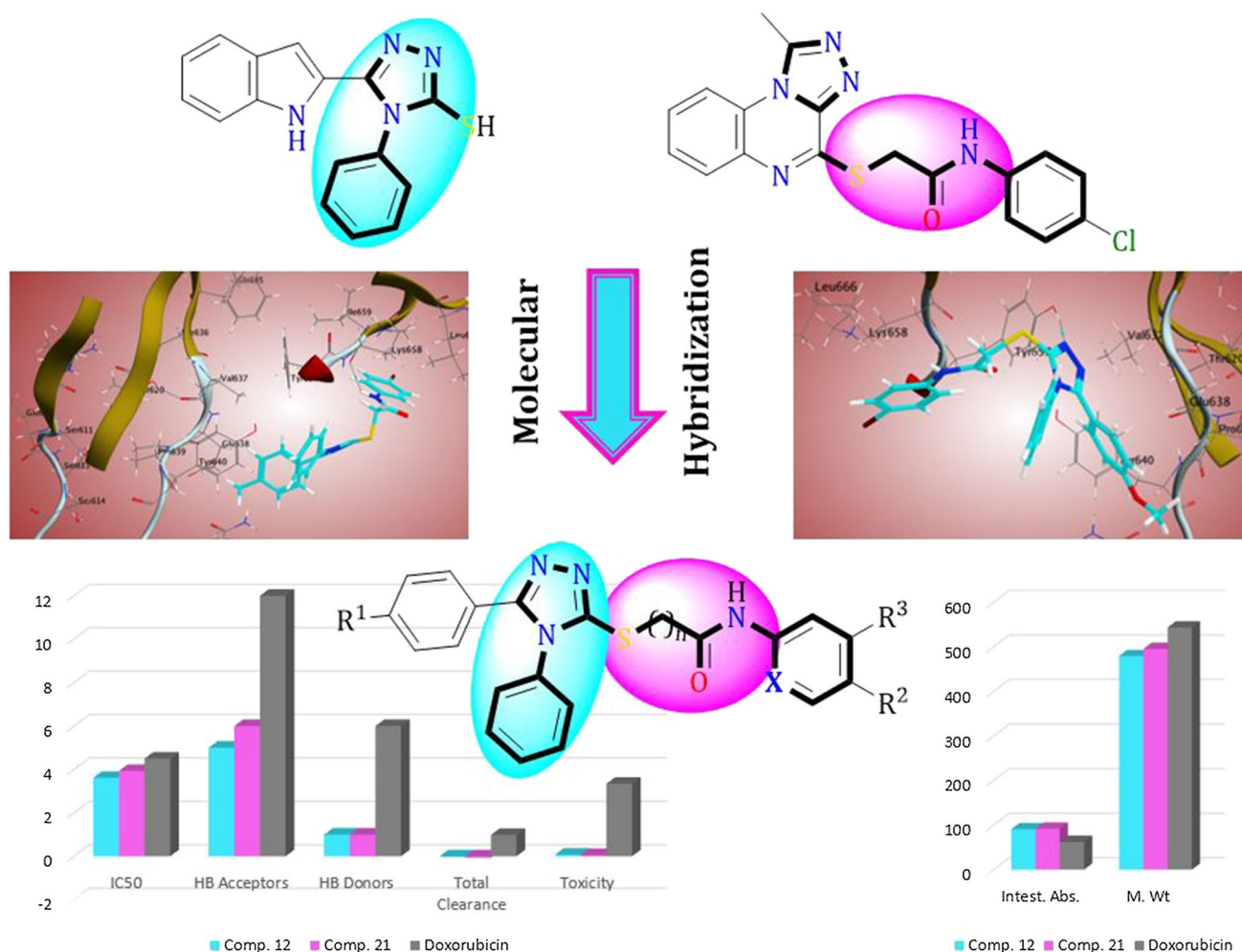
² Pharmaceutical Organic Chemistry Department, College of Pharmacy, Misr University for Science and Technology (MUST), 6th October City, Egypt

³ Department of Pharmaceutical Chemistry, Faculty of Pharmacy, Al-Azhar University, Cairo, Egypt

⁴ Department of Pharmaceutical Chemistry, Faculty of Pharmacy, Heliopolis University for Sustainable Development, Cairo, Egypt

⁵ Pharmaceutical Chemistry Department, Faculty of Pharmacy, Horus University - Egypt, International Coastal Road, New Damietta, Egypt

Graphic abstract



Keywords 1,2,4-Triazoles · Anticancer · STAT3 · Docking · Pharmacokinetic

Introduction

Cancer is characterized by an uncontrolled multiplication of abnormal cells and remains one of the top leading causes of death worldwide. Up to date, more than 150 anticancer agents have been approved [1]. However, severe drug toxicity and resistance of malignant tumors to clinically used drugs are still major obstacles to effective chemotherapeutics, making the urgent need of identifying new anticancer drugs with lower side effects and higher efficacy [2]. The signal transducer and activator of transcription (STAT) proteins are a family of cytoplasmic transcription factors that have the ability to bind with DNA and to induce the transcription of specific genes [3]. Accordingly, they play a crucial role in multiple cellular pathways and are frequently dysregulated or over-expressed

in cancer [4]. Mammals contain seven types of these proteins: STAT1, STAT2, STAT3, STAT4, STAT5a, STAT5b, and STAT6 [5]. Among these seven protein types, STAT3 is a multifunctional member involved in the acute phase response, evolution, cell progression and differentiation, immunity, hematopoiesis, and even tumor survival [6]. STAT3 proteins could be activated by cytokines and growth factors [7]. Upon excitation by cytokines or one of the growth factors, STAT3 is phosphorylated by specific kinases, dimerize, and regulate gene expression by the phosphorylated dimer [8]. While healthy cells display transient physiologic STAT3 activation under the effect of strict regulation by inhibitory molecules, tumor cells depend on the constitutive stimulation of STAT3 for its survival [9]. In addition, the ectopic expression of STAT3 alone is enough for aberrant cell transformation, given

its necessity for tumorigenesis [3]. Consequently, STAT3 proteins have recently emerged as an attractive therapeutic target in the development of anticancer agents [8]. Misregulation of STAT3 signaling pathway leads to its overexpression in different types of malignant cells including the Multidrug-resistant human breast adenocarcinoma (MDA-MB-231) [10, 11] and hepatocellular carcinoma [12, 13].

1,2,4-Triazoles are one of the extremely considerable nitrogen-containing scaffolds in the field of medicinal chemistry because of their diverse biological activities, particularly as anticancer [14–16]. Compounds belonging to this class possess the ability to form a variety of non-covalent interactions with different biological targets through hydrophobic interactions, hydrogen bonding, van der Waals forces, and dipole–dipole interaction [17]. Some 1,2,4-triazole incorporating compounds such as 3-nitro-1,2,4-triazole analogue of [^{18}F]FMISO ([^{18}F]3-NTR, **1**) are currently under clinical evaluation for management of cancer concomitant hypoxia [18]. Also, indolyltriazolethione and 1,2,4-triazole-3-ylthioacetamide derivatives (**2** and **3**) demonstrated significant antiproliferative activity in models of MCF-7 and PC-3 cells, respectively, by activation of apoptosis and increasing the caspase-3 activity [19, 20]. Structural alteration of these scaffolds may result in the identification of new improved chemotherapeutic agents with better pharmacological properties.

Over the past decade, several molecules possessing *N*-arylamide moiety have been synthesized as useful chemotherapeutics with good cytotoxic activity [20–23]. Also, the *N*-arylpropanamide linker has been embedded in many reported compounds with a remarkable anticancer

effect [24, 25]. 1,2,4-Triazole derivatives **4** and **5** with *S*-substituted acetamide moiety (Fig. 1) proved as potential cytotoxic against HT-29 and MDA-MB-231 cell lines, respectively, [15, 22]. Furthermore, an analogous 1,3,4-oxadiazole with an amide linker (compound **6**) has been identified as a STAT3 dimerization inhibitor [26]. Last but not least, compound **7** showed potent anticancer activity and has recently identified as an inhibitor of STAT3 signaling through direct binding with the SH domain in melanoma cancer cells [27].

The resistance of breast cancer against chemotherapeutics remains a major obstacle in the management of such cancer type [28]. MDA-MB-231 cells have been recently documented for their extreme multidrug resistance [28, 29]. Monotherapy for the treatment of breast cancer is insufficient to eradicate the disease, and hence, there is an unmet need for potent combinatorial chemotherapeutics. Hybrid molecules with two or more different pharmacophores may have the potential to decrease the severity of side effects and defeat the drug resistance. Hybrids may also own multiple action mechanisms. It is worth noticing that several hybrid molecules are under different phase clinical trials for the treatment of various diseases including those which are drug-resistant [30], revealing molecular hybridization is a useful strategy to develop novel drugs. Obviously, it is conceivable that molecular hybridization of 1,2,4-triazole framework with the *N*-arylamide or *N*-arylpropanamide has the potential to provide new anticancer candidates with the possibility of lower toxicity and higher efficacy.

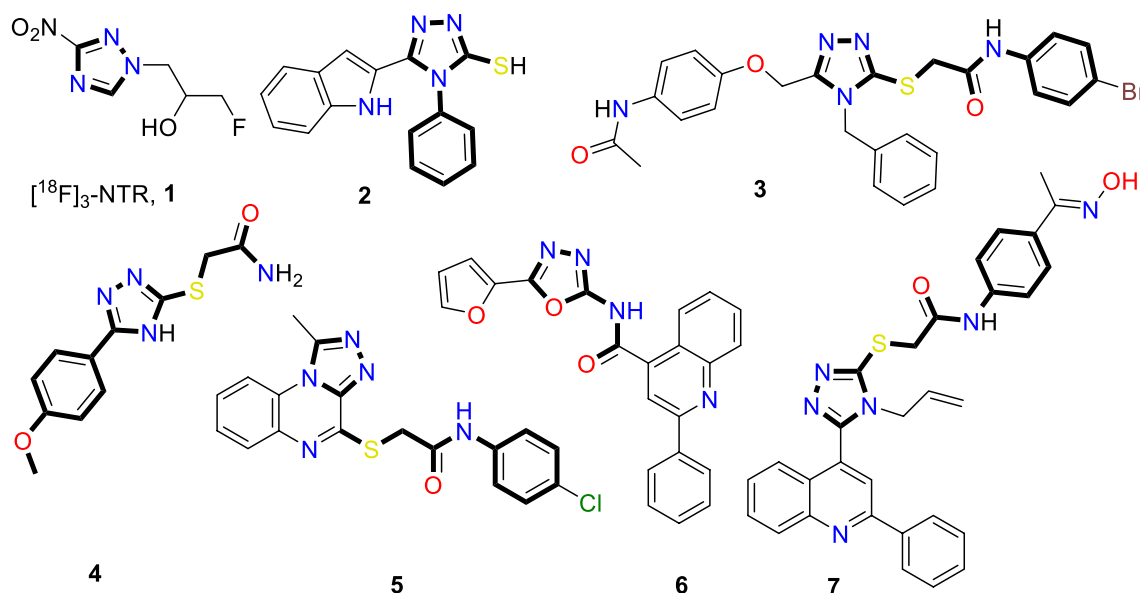


Fig. 1 Structure of representative 1,2,4-triazole and analogous oxadiazole derivatives incorporating *N*-arylamide moieties with potent anticancer and STAT3 inhibitory potential

Rationale and structure-based design

Based on the aforementioned facts and as a continuation of our recent studies [31–33] on identifying new antiproliferative agents, molecular hybridization between 1,2,4-triazole scaffold and the *N*-arylamide or *N*-arylpropanamide moiety was carried out in an attempt to get new anticancer molecules with higher potency and lower toxicity. Molecular hybridization is one of the well-established approaches in drug design which involves the combination of pharmacophores of more than one bioactive molecule [34]. This strategy is expected to produce hybrid structures with improved efficacy and lower toxicity compared to individual parent drugs [35]. Here, inspired by the versatility of the 1,2,4-triazole pharmacophoric ring scaffold and the *N*-arylamide or *N*-arylpropanamide moiety mentioned above, two novel series of hybrid structures of C3-linked 1,2,4-triazole-*N*-arylamide hybrids were designed and synthesized by modifying several structural aspects of the previously reported STAT3 inhibitor (Fig. 2) to evaluate their anticancer activities. Different substitution patterns were introduced to both the phenyl ring at C-5 of the triazole scaffold and the terminal aryl/heteroaryl ring attached with the hydrophilic

N-arylamide linker to investigate the effect of such substitution pattern on the cytotoxicity of the designed compounds. All the synthesized compounds were evaluated for their *in vitro* cytotoxic activity against the chemotherapeutic resistant human breast adenocarcinoma (MDA-MB-231). In addition, the structure–activity relationship of the synthesized compounds was illustrated based on the results of cytotoxicity evaluation. As well, the possible underlying mechanism of the most potent compounds was investigated *in silico* to predict their binding affinity toward the active site of STAT3 as a proposed therapeutic target of their cytotoxic activity. MDA-MB-231 cell line was selected to evaluate the cytotoxicity effect of new compounds after running an *in silico* CLC-prediction to suggest the cytotoxicity against different types of cancer cells. Results of *in silico* cytotoxicity prediction surprisingly showed that one of the top sensitive cell lines to the action of our designed compounds was the breast adenocarcinoma cell line (MDA-MB-231) which has recently documented in a number of articles as a multidrug-resistant cancer cell [28]. To date, doxorubicin remains one of the most commonly prescribed anthracyclines in the treatment of breast cancer, including MDA-MB-231, and hence used as a positive control. In addition, many shreds of

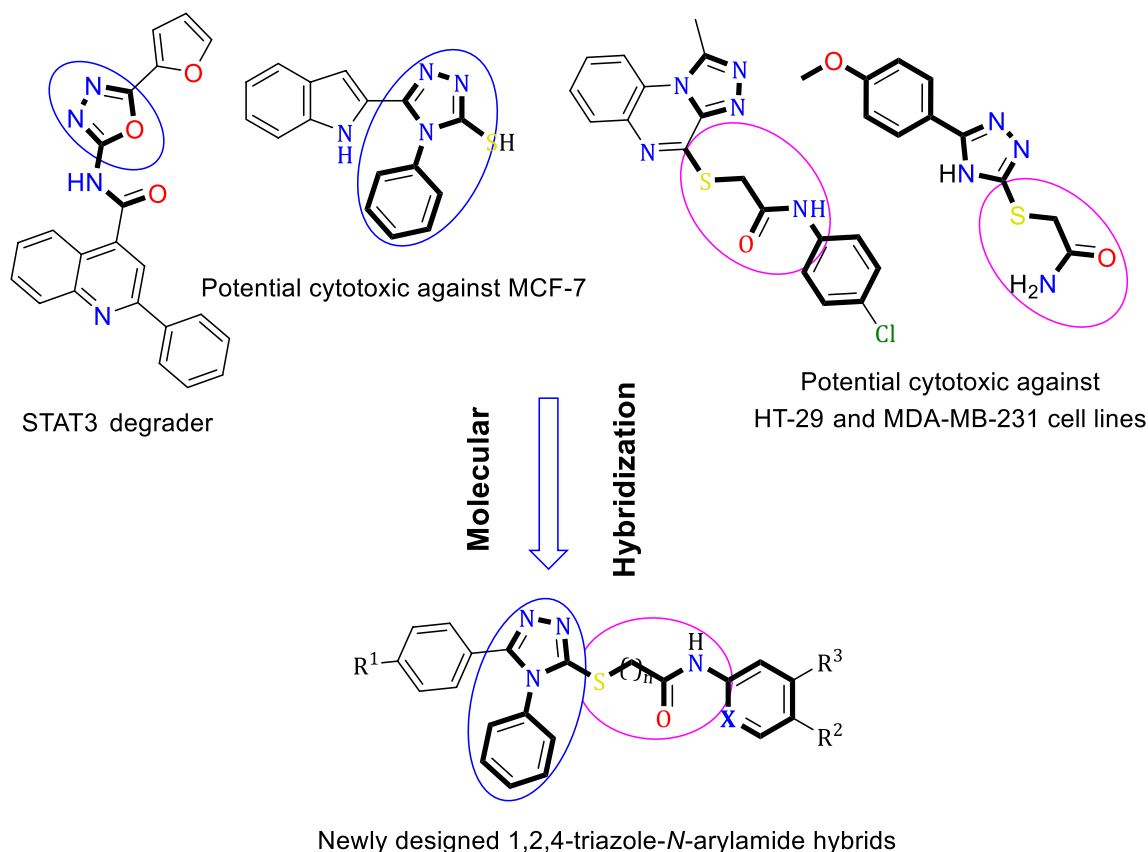


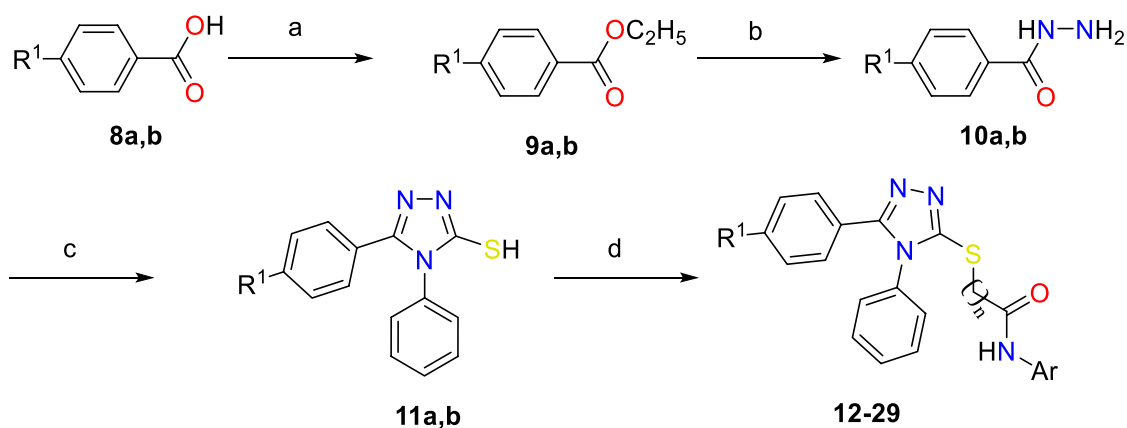
Fig. 2 Molecular hybridization of 1,2,4-triazole scaffold with *N*-arylamide moieties

evidence have recently documented for the overexpression of STAT3 receptors in this type of cancer cells [10, 11]. Consequently, MDA-MB-231 cell line was selected to conduct the in vitro anticancer evaluation and to serve also as a model of STAT3 receptor subtype. Finally, the pharmacokinetic profiles of the highest potent derivatives were examined to evaluate their potential to build up as good drug candidates.

Results and discussion

Chemistry

Final target compounds of the present work were readily achieved in four consecutive steps starting with commercially available *p*-toluic and *p*-methoxybenzoic acids. The general route adopted for the synthesis of the designed 1,2,4-triazole derivatives is outlined in Scheme 1. Our convergent synthesis approach starts with the preparation of *N*-aryl-2-chloroacetamides and *N*-aryl-3-chloropropionamides



Reagents and conditions:

- a)** C₂H₅OH/Conc H₂SO₄, 120 °C, 70-77%; **b)** H₂N-NH₂·H₂O, C₂H₅OH, 80 °C, 90%.
c) 1- C₆H₅NCS/KOH, 120 °C 75-78%; 2- HCl, rt; **d)** Cl(CH₂)_nCONHAr/(C₂H₅)₃N, 90 °C, 70-85%.

Series A, R¹ = CH₃

- 12:** n = 1, Ar = 4-BrC₆H₄
13: n = 1, Ar = 4-ClC₆H₄
14: n = 1, Ar = 4-CH₃C₆H₄
15: n = 1, Ar = 4-OCH₃C₆H₄
16: n = 1, Ar = 1-Naphthyl
17: n = 1, Ar = 2-Pyridinyl
18: n = 1, Ar = 5-Cl-pyridine-2-yl
19: n = 2, Ar = 4-BrC₆H₄
20: n = 2, Ar = 4-OCH₃C₆H₄

Series B, R¹ = OCH₃

- 21:** n = 1, Ar = 4-BrC₆H₄
22: n = 1, Ar = 4-ClC₆H₄
23: n = 1, Ar = 4-CH₃C₆H₄
24: n = 1, Ar = 4-OCH₃C₆H₄
25: n = 1, Ar = 1-Naphthyl
26: n = 1, Ar = 2-Pyridinyl
27: n = 1, Ar = 5-Cl-pyridine-2-yl
28: n = 2, Ar = 4-BrC₆H₄
29: n = 2, Ar = 4-OCH₃C₆H₄

Scheme 1 Synthetic route of the designed new 1,2,4-triazole derivatives

by the reaction of substituted anilines with 2-chloroacetylchloride or 3-chloropropionylchloride in the presence of triethylamine [36, 37]. Substituted benzoic acids **8a, b** converted into their corresponding esters **8a, b** by heating at reflux temperature in absolute ethanol containing a catalytic amount of concentrated sulfuric acid. Nucleophilic substitution of the produced esters with hydrazine hydrate in ethanol [38–40] was carried out to give hydrazide derivatives **10a, b** in relatively good yields and convenient purities. Afterward, the latter hydrazide derivatives were allowed to react with phenyl isothiocyanate under reflux [41, 42] in an alcoholic solution of potassium hydroxide to yield the potassium salts of the prerequisite key intermediates 5-(aryl)-4-phenyl-1,2,4-triazole-3-thiol (**11a, b**). The parent thioalcohols of these potassium salts were readily achieved by the action of dilute hydrochloric acid. Compounds **11a, b** were finally coupled with the appropriate previously prepared 2-chloro-*N*-arylacetamide or 3-chloro-*N*-arylpropanamide derivatives in the presence of triethylamine to complete the synthesis of target compounds **12–29** in relatively reasonable yields and convenient purities.

Progress of chemical reactions was authenticated by TLC methodology, and the final synthesized compounds were purified by column chromatography method. Structures and purities of new sets of 1,2,4-triazol-3-ylthio-*N*-arylacetamide and 1,2,4-triazol-3-ylthio-*N*-arylpropanamide derivatives were confirmed based on their IR, LC–MS, ^1H NMR, and ^{13}C NMR spectral data. Mass spectra of all the new triazole-*N*-arylamide hybrid structures are characterized by the presence of distinctive molecular ion peaks at the

expected m/z value. All the newly synthesized triazoles gave elemental analysis data consistent with that calculated of assigned structures. Collectively, these observations with the disappearance of the SH signals in ^1H NMR spectra of the starting thioles **11a, b** confirmed tethering the amide moiety with triazole nucleus in the final compounds via S-linkage. A reasonable mechanism for the conversion of the hydrazide derivatives **10a, b** into the corresponding 1,2,4-triazole-3-thiols is shown in Fig. 3.

Evaluation of biological activity

Cytotoxicity assay

In order to decipher the cytotoxicity effect of new compounds against different types of cancer cells, in silico CLC-prediction system was used [43]. Using the appropriate in silico technique helps in determining an experiment of high efficiency and reducing cost and implementation time. Results of in silico CLC cytotoxicity prediction surprisingly showed that one of the most susceptible cells to the cytotoxic action of our designed compounds was the multidrug-resistant human breast adenocarcinoma cell (MDA-MB-231). Consequently, MDA-MB-231 cell line was solely selected to conduct the in vitro anticancer evaluation. The in vitro anticancer activity on human breast adenocarcinoma (MDA-MB-231) cancer cell line was performed using MTT assay [44] and doxorubicin as a reference anticancer. Results of preliminary cytotoxic evaluation

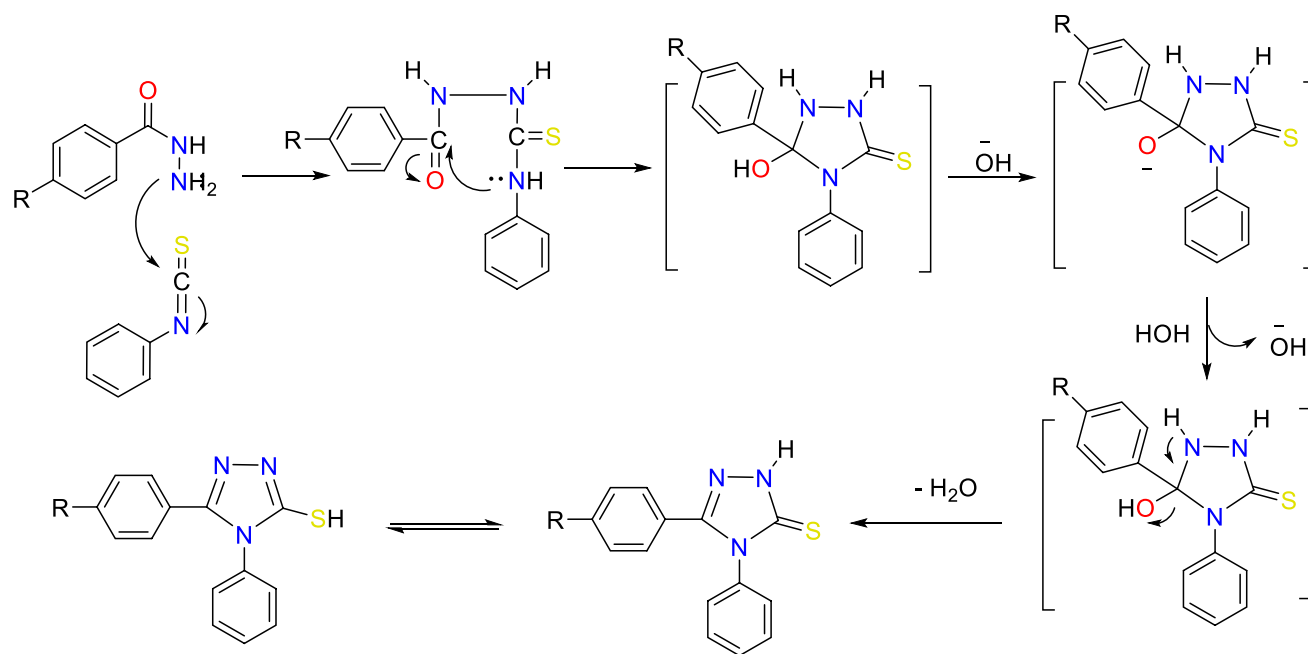
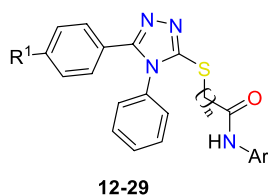


Fig. 3 Proposed reaction mechanism for construction of 4H-1,2,4-triazole-3-thiol

are shown in Table 1. The tabulated results revealed the moderate to good cytotoxic activity of seven derivatives with IC_{50} range of 3.61–17.05 μM . Compounds **12**, **13**, **21**, and **22** were the most potent with either equipotent or even higher potency than that of the standard anticancer drug. Compounds **12** and **21** showed more powerful cytotoxicity effects than doxorubicin with IC_{50} values of 3.61 and 3.93 μM , respectively. Also, compounds **13** and **22** revealed equipotent activity with doxorubicin against the selected cancer cell line with IC_{50} value of 6.44 and 4.55 μM , respectively. Higher doses (up to 87.02 μM) of derivatives **17**, **24**, and **26** were needed for 50% inhibition of cell proliferation, indicating mild activity of these derivatives.

Table 1 In vitro anticancer activity of the designed 1,2,4-triazoles against human breast adenocarcinoma (MDA-MB-231) cancer cell line



Cpd.	R ¹	Ar	n	IC_{50} (μM)* MDA-MB-231
12.	CH₃	4-BrC₆H₄	1	3.61 ± 0.56
13.	CH ₃	4-ClC ₆ H ₄	1	6.44 ± 1.36
14.	CH ₃	4-CH ₃ C ₆ H ₄	1	> 100
15.	CH ₃	4-OCH ₃ C ₆ H ₄	1	10.96 ± 0.65
16.	CH ₃	1-Naphthyl	1	> 100
17.	CH ₃	2-Pyridinyl	1	77.60 ± 0.96
18.	CH ₃	5-Cl-pyridine-2-yl	1	16.21 ± 1.41
19.	CH ₃	4-BrC ₆ H ₄	2	> 100
20.	CH ₃	4-OCH ₃ C ₆ H ₄	2	> 100
21.	OCH₃	4-BrC₆H₄	1	3.93 ± 0.27
22.	OCH₃	4-ClC₆H₄	1	4.55 ± 0.55
23.	OCH ₃	4-CH ₃ C ₆ H ₄	1	> 100
24.	OCH ₃	4-OCH ₃ C ₆ H ₄	1	87.02 ± 1.17
25.	OCH ₃	1-Naphthyl	1	> 100
26.	OCH ₃	2-Pyridinyl	1	47.91 ± 0.72
27.	OCH₃	5-Cl-pyridine-2-yl	1	17.05 ± 1.01
28.	OCH ₃	4-BrC ₆ H ₄	2	> 100
29.	OCH ₃	4-OCH ₃ C ₆ H ₄	2	> 100
Doxorubicin				4.50 ± 0.26

Bold values indicate compounds with good activity and binding affinity
 *Cytotoxicity was assayed by treating cells with the test compound for 72 h and expressed as the concentration needed to inhibit 50% of tumor cell proliferation (IC_{50}). Data here are presented as the means of five independent experiments ± SD

Structure–activity relationship study

As mentioned before, the investigation of structure–activity relationship of newly synthesized triazoles as anticancer agents is one of the main objectives of this work. SAR study of new compounds revealed several common findings: (1) The nature of the substituent group at C-5 had no considerable impact on the activity against the tested cancer cell line. Generally, compounds **12–20**, incorporating a *para*-tolyl substituent group at C-5 and compounds **21–29**, incorporating *para*-methoxyphenyl substituent group at C-5, revealed equipotent activity regardless of the nature of the *para* substituent; (2) conversely, the electronic nature of the terminal aryl ring of lipophilic tail presented a considerable influence on the cytotoxicity. Compounds incorporating hydrogen bonding acceptor fragments attached to the terminal aryl ring displayed potent antitumor activity against the tested cell line compared with other derivatives; (3) compounds possessing monocyclic aryl substituent attached with the acetamide linker at C-3 of the triazole core structure, such as derivatives **12**, **13**, **15**, **21**, **18**, **22**, and **27**, exhibited remarkable and potent antitumor activity (IC_{50} = 3.61–17.05 μM) compared with similar compounds bearing naphthyl moieties attached with the hydrophilic linkers, such as derivatives **16** and **25** (IC_{50} values > 100 μM). Exceptionally, 2-((4-phenyl-5-(*p*-tolyl)-4*H*-1,2,4-triazol-3-yl)thio)-*N*-(pyridin-2-yl)acetamide (**17**) is approximately twofold less potent (IC_{50} = 87.02 μM) against the tested cancer cell than the analogous 2-((5-(4-methoxyphenyl)-4-phenyl-4*H*-1,2,4-triazol-3-yl)thio)-*N*-(pyridin-2-yl)acetamide (**26**), which displayed IC_{50} value of 47.91 μM . Incorporation of the isosteric pyridyl ring instead of the phenyl, as in case of **17**, **18**, **26**, and **27** led to slight decrease in antitumor activity (IC_{50} values, 17.05–77.60 μM); (4) the structure activity relationships suggested that all compounds with an *N*-arylacetamide moiety on C-3 position displayed better cytotoxic activity than those substituted by *N*-arylpropanamide on the same position. A summary of the structure–activity relationship is presented in Fig. 4.

Molecular docking study

In the present work, a docking study was performed to elucidate the binding modes of all the designed compounds inside the binding pocket of the signal transducer and activator of transcription 3 (PDB ID: 6NJS). Docking study was conducted using the MOE 2014.09 software to determine the free energy and binding mode. Selection of the best promising derivatives depended on both the perfect binding mode and the highest free energy of binding. The lowest value of binding energy depicts the best conformational position of the ligand within the active site of the target protein. Free energies of binding of all new compounds and the

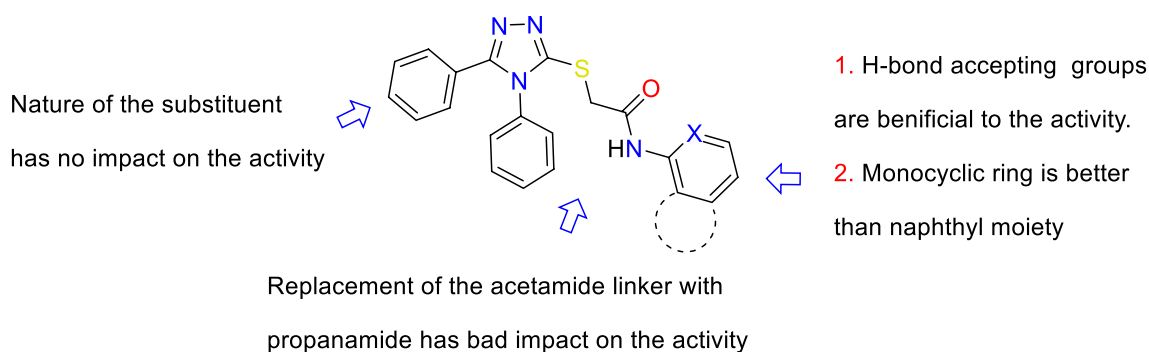


Fig. 4 Summary of SAR study of the synthesized 1,2,4-triazoles

Table 2 The binding free energies (ΔG , kcal/mol) of the target triazoles and the co-crystallized ligand (SD-36) with the binding site STAT3

Compound	ΔG (kcal/mol)	Compound	ΔG (kcal/mol)
12.	-6.94	22.	-7.09
13.	-7.14	23.	-6.30
14.	-6.12	24.	-6.24
15.	-6.67	25.	-6.11
16.	-6.09	26.	-6.32
17.	-6.07	27.	-6.77
18.	-6.34	28.	-6.14
19.	-6.01	29.	-5.95
20.	-5.97	SD-36	-8.25
21.	-6.98		

Bold values indicate compounds with good activity and binding affinity

co-crystallized ligand (SD-36), a STAT3 degrader, are presented in Table 2. Binding mode of the co-crystallized ligand SD-36 with the pocket of signal transducer and activator of transcription 3 exhibited a binding energy of -8.25 kcal/mol. According to Bai et al. [45], key interactions for SD-36 degrader of STAT3 are as follows: (a) an extensive hydrogen bonding network between the phosphoric acid moiety of SD-36 and the side chains of Arg609, Ser611, and Ser613; (b) the fluorine atom of the difluoromethyl group forms a hydrogen bond with Arg609; (c) two hydrogen bonding interactions between the glutamine C=O and NH of SD-36 and Gln644 and Tyr640; (d) water-mediated hydrogen bonds with the Tyr640's OH and amide nitrogen of Lys658. From the new compounds docked in STAT3, *N*-arylacetamides with monocyclic aryl rings showed adequate spatial orientations and distinct interaction patterns with the target enzyme compared to other analyzed structures. As displayed in Table 2, all the target compounds comprise the same scaffold (1,2,4-triazol-3-ylthio)-*N*-arylamide, but only the changes are mainly in both the length of amide linkers and

para-substituents of terminal aryl rings attached with the amide linkers. In fact, compounds other than **12**, **13**, **15**, **18**, **21**, **22**, and **27**, which have low activity, ($IC_{50} \geq 47.91 \mu M$) all either do not contain hydrogen bond acceptor at *para* positions in amide functional group or the linker is propanamide, while compounds **12**, **13**, **15**, **18**, **21**, **22**, and **27** (IC_{50} 3.61–17.05 μM) have bromo, chloro, or methoxy substituents at *para* positions and the linker is acetamide rather than propanamide.

As a result, compounds that hold a hydrogen bond acceptor group possess good inhibitory activity. From the in vitro study, we suggested that the compounds **12**, **13**, **21**, and **22** with hydrogen bond acceptor group at *para*-positions in acetamide functionality display much higher activity than other compounds. These compounds form key interactions similar to the reported STAT3 degrader with the amino acids Gln644, Tyr640, and Lys658. Binding modes of compounds **12** and **13** in series A, as representative examples of triazoles with hydrogen bond acceptors at the *para* position of the terminal benzene ring, exhibited affinity values of -6.94 and 7.14 kcal/mol, respectively. Obeying almost the same interaction pattern of co-crystallized ligand SD-36, the docked pose of **12** was stabilized by hydrogen bond of the NH with Lys658 residue. The phenyl ring at C-5 has involved in a sidewise arene-H interaction with Gln644 and Tyr640 residues. Carbonyl group of compound **13** showed an additional hydrogen bonding interaction with Tyr657 residue (Fig. 5). Similarly, compounds **21** and **22** as representative examples of series B showed similar binding modes with that of SD-36, with affinity value of -6.98 and 7.09 kcal/mol, respectively. The N-1 of triazole ring played as a hydrogen bond acceptor with the carboxylic group of Tyr657 and Glu638 residues. The terminal phenyl rings formed arene-H interactions with Lys658 and Pro639 residues.

Compounds **18** and **27**, as examples of derivatives incorporating pyridyl moiety attached with acetamide linkers, exhibited different virtual binding mode with that of SD-36. Compound **18** revealed an affinity value of -6.34 kcal/mol and showed three different interactions with the binding site

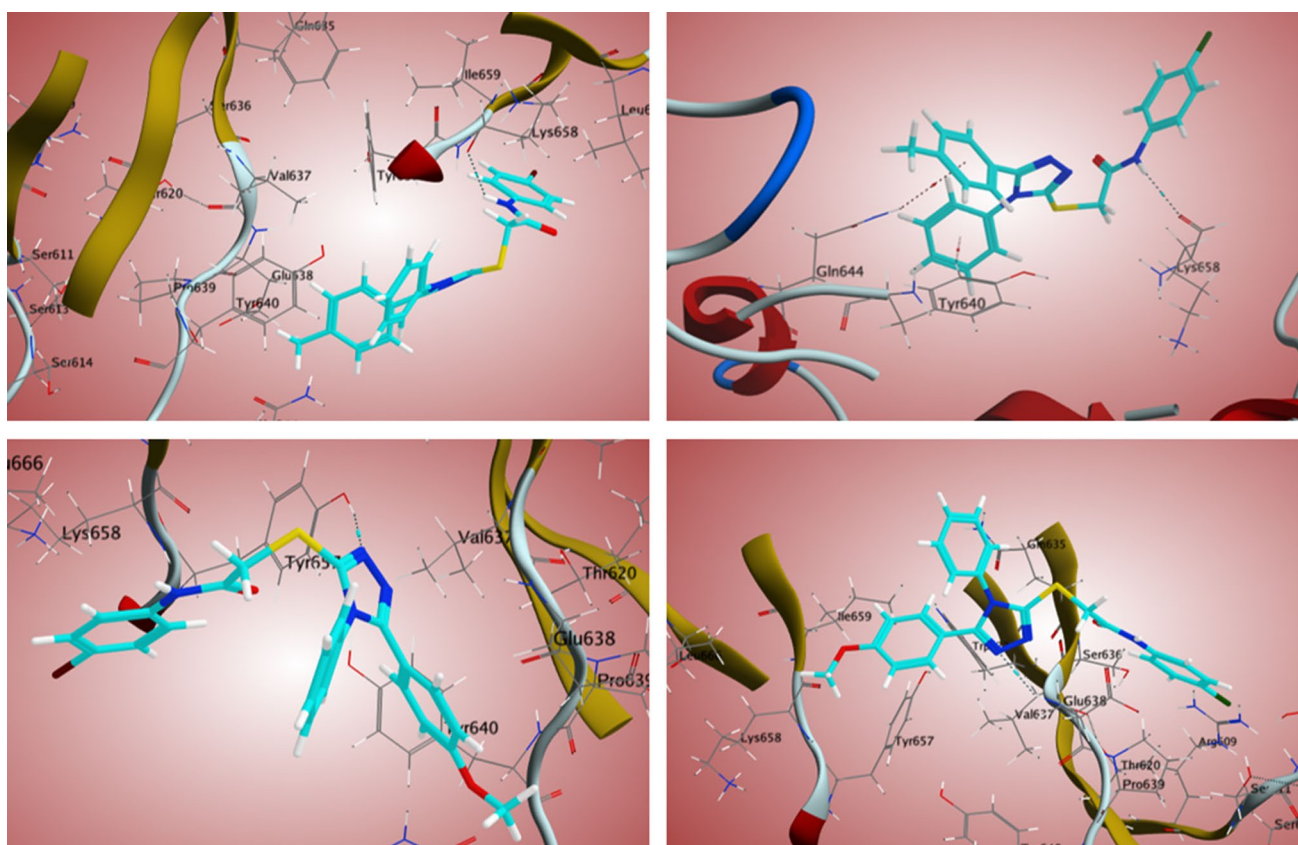


Fig. 5 3D interactions of compounds **12** (upper left panel), **13** (upper right panel), **21** (lower left panel), and **22** (lower right panel) with the active site of STAT3 (PDB ID: 6NJS)

of STAT3. These interactions involve two arene-H interactions between the pyridine and triazole rings in the target compounds and Pro639 and Tyr657 residues in STAT3, respectively. The last interaction is in the form of a hydrogen bond between the NH of acetamide linker with the carbonyl oxygen of Ser636 residue.

Increasing the linker length at the C-3 position as in compounds **19**, **20**, **28**, and **29** displayed an undesirable effect on the affinity for the receptor (Table 2). Also, replacing the phenyl and pyridyl rings at C-3 with naphthyl moiety, as in compounds **16** and **25**, showed a similar unfavorable effect on the affinity. In addition, the presence of such a bulky substituent at C-3 may decrease the affinity of the last two compounds due to failure of these compounds to accommodate the binding pocket of the receptor and thus the scaffold pushed out of the catalytic domain. The obtained result for compound **16** is virtually the same as that of compound **25**. With -6.19 kcal/mol free energy of binding, the binding mode of **16** involves three arene-H interactions between the triazole, phenyl, and naphthyl rings with Gln644, Tyr657, and Glu638 residues, respectively.

Collectively, the obtained results of binding free energies (ΔG) and binding studies were consistent with results

of in vitro cytotoxicity data. These results indicated that except for **16** and **25**, all the studied triazole derivatives with *N*-arylamide moiety revealed similar positions and orientations inside the binding site of the STAT3. The introduction of either a longer linker or a bulky aromatic ring, like naphthalene, both decrease the affinity of the compound for the STAT3 receptor. In addition, the results explain that some of these compounds may have good binding affinities to the receptor and the computed values reflect the overall trend. Furthermore, the present work spotlighted the triazole moiety as an attractive scaffold for obtaining potent STAT3 inhibitor.

Pharmacokinetic profiling study

In the present study, an in silico computational study of the representative C3-linked 1,2,4-triazole-*N*-arylamide hybrids was performed for determining the surface area and other physicochemical properties following the directions of Lipinski's rule of five [46]. Lipinski suggested that the absorption of an orally administered compound is more likely to be better if the molecule satisfies at least three of the following rules: (1) H bond donors (OH, NH, and SH) ≤ 5 ;

(2) H bond acceptors (N, O, and S atoms) ≤ 10 ; (3) molecular weight < 500 ; (iv) $\log P < 5$. Compounds violating more than one of these rules could not have good bioavailability. While the reference anticancer drug doxorubicin violated three of Lipinski's rules, all the highest active derivatives in this study violated only one (LogP) except **15** which, gratifyingly, satisfied all the Lipinski's rules. All derivatives have a number of hydrogen bond acceptors between 5 and 6 and only 1 hydrogen bond donor, and these values agree with Lipinski's rules.

Also, absorption, distribution, metabolism, excretion, and toxicity (ADMET) profiles of the new synthesized 1,2,4-triazole-*N*-arylamide hybrids were tentatively evaluated to analyze its potential to build up as good oral drug candidates. The compound's pharmacokinetic profile detects how it would be absorbed, distributed, metabolized, and excreted (ADME). While optimal binding of a drug with its therapeutic protein target is critical, ensuring that it will arrive this target in an adequate concentration to produce the biological effect is also essential. Prediction of ADMET profiles is conducted using the pkCSM descriptors algorithm protocol [47]. Two main structural features correlate properly with PK properties, the two-dimensional polar surface area (PSA_{2D}) and the lipophilicity levels (LogP). Absorption of a drug depends on a number of factors including membrane permeability, intestinal absorption, skin permeability, and P-glycoprotein substrate or inhibitor. Drug distribution depends on the volume of distribution (VD_{ss}), the blood brain barrier permeability (logBB), and CNS permeability. Metabolism is predicted depending on the CYP models for substrate or inhibition. Excretion is predicted based on the total clearance and the renal OCT2 substrate. Toxicity of the drugs is predicted depended on AMES toxicity, hERG inhibition, hepatotoxicity, and skin sensitization. These parameters were all calculated for the highest potent triazoles **12**, **13**, **15**, **18**, **21**, and **22** as well as to reference marketed anticancer drug doxorubicin. After calculating the ADMET properties (Table 3), we can suggest that the highest potent derivatives have the preference of better intestinal absorption in human over doxorubicin (90.842–93.166) compared with 62.372 in case of doxorubicin. This advantage is attributed to the greater lipophilicity of the designed ligands, which would make it easy to go along biological membranes [48]. Accordingly, they may have considerable good bioavailability after oral administration in experimental testing. Analyzing the CNS permeability, *N*-arylamide derivatives **12** and **13** displayed the highest ability to penetrate the CNS (CNS permeability > -2.0), while doxorubicin is unable to penetrate (CNS permeability < -4.0). It was also clear that in contrast to doxorubicin, all compounds could inhibit the cytochrome P3A4, the main cytochrome involved in drug metabolism. This is possibly due to the higher lipophilicity of our designed ligands. The excretion was evaluated

in terms of the total clearance, a parameter related to the bioavailability, and is significant in deciding dose intervals. Produced data demonstrated that **15** and doxorubicin revealed the highest total clearance values (0.143 and 0.987, respectively), when compared to other ligands, especially **21**, which showed the lowest total clearance value (-0.066). Thus, **15** and doxorubicin could be excreted faster and consequently require shorter dosing intervals. Unlike doxorubicin, compound **21** showed a slower clearance rate, which means the preference of longer dosing intervals for the later. The last parameter analyzed in the pharmacokinetic profile of our newly synthesized triazoles is the hepatotoxicity. As shown in Table 3, all new ligands as well as doxorubicin shared the drawback of hepatotoxic effects. Gratifyingly, our designed compounds showed better tolerability (~ 0.88) compared with 0.081 for doxorubicin. Finally, the oral acute toxic doses of the designed compounds (LD₅₀) are higher than those of the reference drug (~ 2.80 compared with 2.40).

Conclusion

In the present study, we are reporting the design, synthesis, in vitro anticancer evaluation, of 1,2,4-triazole-*N*-arylamide hybrids in a model of MDA-MB-231 cell line. In silico docking and pharmacokinetic profiling studies were also conducted to determine the potential of new compounds to build up as good oral drug candidates. Our target compounds were designed based on molecular hybridization of the 1,2,4-triazole scaffold of [¹⁸F]3-NTR with *N*-arylamide moiety presented in a wide variety of anticancer agents. The possible underlying mechanism of action of the highest active derivatives was explained in terms of the in silico binding affinity toward STAT3 receptor as a proposed potential therapeutic target. This study led us to the identification of four novel C3-linked 1,2,4-triazole-*N*-arylamide hybrids of interesting antiproliferative activity against the multidrug-resistant human breast adenocarcinoma cells (MDA-MB-231) at low micromolar concentration, and probable STAT3 inhibitory potentials. Further research is in progress to identify the accurate mechanisms through which triazole-*N*-arylamide may impact antiproliferative activity and to elucidate in depth the structure–activity relationships after more cavernous structure optimization.

Experimental section

General

Melting points were measured using electrothermal (Stuart SMP30) apparatus and were uncorrected. Infrared spectra

Table 3 ADMET profile of the six most active compounds and doxorubicin

Parameter	12	13	15	18	21	22	Dox.
<i>Molecular properties</i>							
Molecular weight	479.403	434.952	430.533	435.94	495.402	450.951	543.525
LogP	5.73602	5.62692	4.98212	5.02192	5.4362	5.3271	0.0013
Rotatable bonds	6	6	7	6	7	7	5
Acceptors	5	5	6	6	6	6	12
Donors	1	1	1	1	1	1	6
Surface area	187.226	183.662	184.837	182.882	192.340	188.776	222.081
<i>Absorption</i>							
Water solubility	-5.178	-5.158	-4.699	-4.377	-4.635	-4.619	-2.915
Caco2 permeability	0.978	0.98	1.066	1.106	1.067	1.07	0.457
Intestinal abs. (human)	90.842	90.909	93.386	93.166	92.024	92.091	62.372
Skin Permeability	-2.736	-2.736	-2.736	-2.736	-2.736	-2.736	-2.735
P-glycoprotein substrate	Yes	Yes	Yes	No	Yes	Yes	Yes
P-glycoprotein I inhibitor	Yes	Yes	Yes	Yes	Yes	Yes	No
P-glycoprotein II inhibitor	Yes	Yes	Yes	Yes	Yes	Yes	No
<i>Distribution</i>							
VD _{ss} (human)	-0.038	-0.052	-0.162	0.069	-0.105	-0.118	1.647
Fraction unbound (human)	0.216	0.216	0.238	0.238	0.23	0.23	0.215
BBB permeability	0.311	0.312	-0.42	-0.736	-0.591	-0.583	-1.379
CNS permeability	-1.73	-1.752	-2.061	-2.11	-2.012	-2.035	-4.307
<i>Metabolism</i>							
CYP2D6 substrate	No						
CYP3A4 substrate	Yes	Yes	Yes	Yes	Yes	Yes	No
CYP1A2 inhibitor	Yes	Yes	Yes	Yes	Yes	No	No
CYP2C19 inhibitor	Yes	Yes	Yes	Yes	Yes	Yes	No
CYP2C9 inhibitor	Yes	Yes	Yes	Yes	Yes	Yes	No
CYP2D6 inhibitor	No						
CYP3A4 inhibitor	Yes	Yes	Yes	Yes	Yes	Yes	No
<i>Excretion</i>							
Total clearance	-0.042	-0.021	0.143	0.081	-0.066	-0.044	0.987
Renal OCT2 substrate	No						
<i>Toxicity</i>							
AMES toxicity	No	Yes	No	No	No	No	No
Max. tolerated dose (human)	0.893	0.892	0.879	0.900	0.896	0.895	0.081
hERG I inhibitor	No						
hERG II inhibitor	Yes						
Oral rat acute toxicity (LD ₅₀)	2.899	2.901	2.921	2.795	2.913	2.914	2.408
Oral rat chronic toxicity (LOAEL)	0.078	0.088	0.367	0.297	0.057	0.068	3.339
Hepatotoxicity	Yes						
Skin sensitization	No						
T. Pyriformis toxicity	0.286	0.286	0.286	0.286	0.286	0.286	0.285
Minnow toxicity	-0.287	-0.141	-0.583	-1.286	-0.771	-0.625	4.412

were recorded on Pye Unicam SP 1000 IR spectrophotometer at the Pharmaceutical Analytical Unit, Faculty of Pharmacy, Al-Azhar University. ¹H NMR and ¹³C NMR spectra were recorded in DMSO-*d*₆ at 300 and 100 MHz, respectively, on a Varian Mercury VXR-300 NMR spectrometer at NMR Lab, Faculty of Science, Cairo University. Chemical shifts were related to that of the solvent, and TMS was

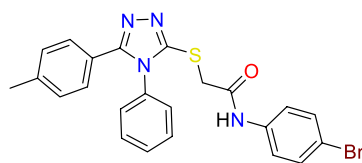
used as an internal standard. Coupling constant and chemical shift values are mentioned in Hz and ppm, respectively. Mass spectra and elemental analyses were carried out at the Regional Center for Mycology and Biotechnology, Al-Azhar University, Cairo, Egypt. The progress of reactions was monitored with Merck silica gel IB2-F plates (0.25 mm thickness) and was visualized under a UV lamp using

different solvent systems as mobile phases. Reagents and starting benzoic acid derivatives, hydrazine hydrate, phenyl isothiocyanate, chloroacetyl chloride, chloropropionyl chloride, 2-aminopyridine, 5-chloropyridine-2-amine, and aniline derivatives were purchased from Aldrich chemical company and were used as received. 2-Chloro-*N*-arylacetyl amides and 3-chloro-*N*-arylpropanamides were prepared following reported procedures [25, 39]. Compounds **11a**, **b** were synthesized according to the direction of reported procedures [16, 27, 49].

General procedures for synthesis of *N*-aryl-3-((4-phenyl-5-(aryl)-4*H*-1,2,4-triazol-3-yl)thio)acetamide/propanamide derivatives (12–29)

As displayed in Scheme 1, the appropriate 5-(aryl)-4-phenyl-4*H*-1,2,4-triazole-3-thiol derivatives **11a**, **b** (0.001 mol) was suspended in a solution of triethylamine (0.025 mol) in DMF (30 mL). The right 2-chloro-*N*-arylacetyl amide or 3-chloro-*N*-arylpropanamide derivative (0.011 mol) was added, and the reaction mixture was heated to 90 °C for 8 h with continuous stirring. After the reaction was completed (monitored by TLC), the mixture was allowed to cool and to stand overnight. Later, after adding distilled cold water (100 mL), the obtained solid products were collected through filtration, washed with three portions of cold water (100 mL each) to remove the side salt product triethylammonium chloride, dried, crystallized from ethanol, and finally purified by using column chromatography technique using hexane–ethyl acetate as an eluent to afford pure 1,2,4-triazole derivatives (**12–29**) in reasonable yields.

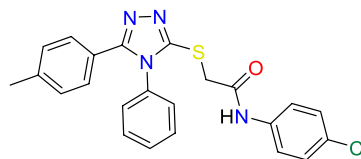
N-(4-Bromophenyl)-2-((4-phenyl-5-(*p*-tolyl)-4*H*-1,2,4-tria-



zol-3-yl)thio)acetamide (12) White solid (0.35 g, 73%); mp = 242–244 °C; IR (KBr) ν_{\max} cm^{-1} : 3431 (NH), 3012 (CH aromatic), 2984 (CH aliphatic), 1675 (C=O), 1556 (C=C); ^1H NMR (DMSO- d_6) δ : 10.49 (brs, 1H, NH), 7.55–7.40 (m, 9H), 7.23–7.13 (m, 4H), 4.17 (s, 2H, SCH₂), 2.26 (s, 3H, CH₃); ^{13}C NMR (DMSO- d_6) δ : 166.4, (C=O), 154.3, (triazole C-5), 151.7, (triazole C-3), 151.3, (*N*-phenyl C-1), 148.2, (*NH*-phenyl C-1), 139.5, (phenyl C-4, *N*-phenyl C-4), 138.3, (phenyl C-1), 133.8, (*NH*-phenyl C-3, C-5), 130.0, (phenyl C-3, C-5), 129.9, (*N*-phenyl C-3, C-5), 129.1, (*NH*-phenyl C-4), 127.7, (*N*-phenyl C-2, C-6), 127.2, (*NH*-phenyl C-2, C-6), 123.6, (phenyl C-2, C-6), 36.8, (SCH₂), 20.8, (CH₃); MS (m/z , %): 479 (M+, 1.15%), 481 (M+2, 0.91%).

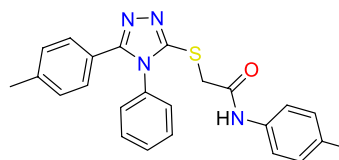
Anal. Calc. for C₂₃H₁₉BrN₄OS (M.W. = 479): C, 57.63; H, 4.00; N, 11.69; Found: C, 57.75; H, 4.14; N, 11.80%.

N-(4-Chlorophenyl)-2-((4-phenyl-5-(*p*-tolyl)-4*H*-1,2,4-tria-



zol-3-yl)thio)acetamide (13) White solid (0.36 g, 83%); mp = 235–237 °C; IR (KBr) ν_{\max} cm^{-1} : 3428 (NH), 3078 (CH aromatic), 2961 (CH aliphatic), 1676 (C=O), 1520 (C=C); ^1H NMR (DMSO- d_6) δ : 10.49 (brs, 1H, NH), 7.60 (d, J = 8.4 Hz, 2H), 7.55 (t, J = 8.4 Hz, 1H), 7.41 (d, J = 9.6 Hz, 2H), 7.36 (d, J = 8.8 Hz, 2H), 7.23 (t, J = 8.0 Hz, 2H), 7.15 (d, J = 7.2 Hz, 2H), 7.13 (d, J = 7.2 Hz, 2H), 4.17 (s, 2H, SCH₂), 2.26 (s, 3H, CH₃); ^{13}C NMR (DMSO- d_6) δ : 165.5, (C=O), 154.4, (triazole C-5), 151.6, (triazole C-3), 151.1, (*N*-phenyl C-1), 148.0, (*NH*-phenyl C-1), 139.5, (*NH*-phenyl C-4), 138.2, (phenyl C-1, C-4), 133.8, (*NH*-phenyl C-3, C-5), 130.0, (phenyl C-3, C-5), 125.3, (*NH*-phenyl C-2, C-6), 123.6, (*N*-phenyl C-3, C-5), 120.6, (phenyl C-2, C-6), 119.6, (*N*-phenyl C-4), 113.3, (*N*-phenyl C-2, C-6), 36.7, (SCH₂), 20.7, (CH₃); MS (m/z , %): 434 (M+, 8.84%), 436 (M+2, 2.061%). Anal. Calc. for C₂₃H₁₉ClN₄OS (M.W. = 454): C, 63.51; H, 4.40; N, 12.88; Found: C, 62.51; H, 4.47; N, 13.01%.

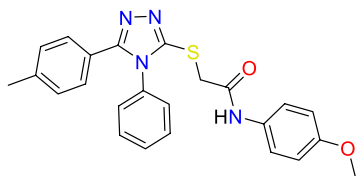
2-((4-Phenyl-5-(*p*-tolyl)-4*H*-1,2,4-triazol-3-yl)thio)-*N*-(*p*-tolyl)



acetamide (14) White solid (0.28 g, 68%); mp = 227–229 °C; IR (KBr) ν_{\max} cm^{-1} : 3422 (NH), 3070 (CH aromatic), 2988 (CH aliphatic), 1670 (C=O), 1461 (C=C); ^1H NMR (DMSO- d_6) δ : 10.23 (brs, 1H, NH), 7.55 (d, J = 1.6 Hz, 2H), 7.54 (t, J = 2.0 Hz, 1H), 7.45 (d, J = 7.6 Hz, 2H), 7.43 (d, J = 8.4 Hz, 2H), 7.41 (t, J = 3.6 Hz, 2H), 7.22 (d, J = 8.0 Hz, 2H), 7.10 (d, J = 8.8 Hz, 2H), 4.15 (s, 2H, SCH₂), 2.26 (s, 6H, 2CH₃); ^{13}C NMR (DMSO- d_6) δ : 170.6, (C=O), 154.3, (triazole C-5), 151.0, (triazole C-3), 144.2, (*N*-phenyl C-1), 139.4, (*NH*-phenyl C-1), 133.8, (phenyl C-4, *N*-phenyl C-4), 132.7, (phenyl C-1), 130.0, (*NH*-phenyl C-3, C-5), 129.9, (phenyl C-3, C-5), 129.3, (*N*-phenyl C-3, C-5), 128.5, (*N*-phenyl C-4), 127.7, (*N*-phenyl C-2, C-6), 127.5, (*NH*-phenyl C-2, C-6), 123.7, (phenyl C-2, C-6), 38.5, (SCH₂), 21.1, (CH₃), 20.7, (CH₃); MS (m/z , %): 414 (M+, 3.12%). Anal. Calc. for C₂₄H₂₂N₄OS (M.W. = 414):

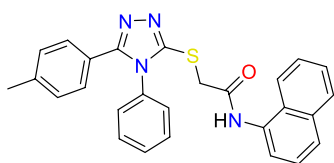
C, 69.54; H, 5.35; N, 13.52; Found: C, 69.58; H, 5.51; N, 13.57%.

***N*-(4-Methoxyphenyl)-2-((4-phenyl-5-(*p*-tolyl)-4*H*-1,2,4-tri-**



azol-3-yl)thio)acetamide (15) White solid (0.33 g, 77%); mp = 223–225 °C; IR (KBr) ν_{\max} cm^{-1} : 3431 (NH), 3056 (CH aromatic), 2945 (CH aliphatic), 1680 (C=O), 1440 (C=C); ^1H NMR (DMSO- d_6) δ : 9.83 (brs, 1H, NH), 7.52 (d, J = 3.0 Hz, 2H), 7.48 (d, J = 9.3 Hz, 1H), 7.44 (d, J = 9.3 Hz, 2H), 7.25 (d, J = 8.1 Hz, 2H), 7.15 (t, J = 8.1 Hz, 2H), 6.87 (d, J = 9.3 Hz, 2H), 6.84 (d, J = 9.3 Hz, 2H), 3.71 (s, 2H, SCH_2), 2.82 (s, 3H, OCH_3), 2.27 (s, 3H, CH_3); ^{13}C NMR (DMSO- d_6) δ : 168.4, (C=O), 160.1, (triazole C-5), 155.1, (triazole C-3), 151.1, (*N*-phenyl C-1), 134.0, (NH-phenyl C-1), 132.1, (phenyl C-4, *N*-phenyl C-4), 129.9, (phenyl C-1), 129.8, (NH-phenyl C-3, C-5), 129.3, (phenyl C-3, C-5), 127.7, (*N*-phenyl C-3, C-5), 120.5, (*N*-phenyl C-4), 118.9, (*N*-phenyl C-2, C-6), 114.0, (NH-phenyl C-2, C-6), 113.7, (phenyl C-2, C-6), 55.2, (OCH_3), 35.8, (SCH_2), 21.8, (CH_3); MS (m/z , %): 430 (M^+ , 10.29%). Anal. Calc. for $\text{C}_{24}\text{H}_{22}\text{N}_4\text{O}_2\text{S}$ (M.W. = 430): C, 66.96; H, 5.15; N, 13.01; Found: C, 66.99; H, 5.19; N, 13.12%.

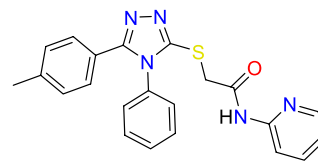
***N*-(Naphthalen-1-yl)-2-((4-phenyl-5-(*p*-tolyl)-4*H*-1,2,4-tri-**



azol-3-yl)thio)acetamide (16) White solid (0.31 g, 69%); mp = 231–233 °C; IR (KBr) ν_{\max} cm^{-1} : 3451 (NH), 3031 (CH aromatic), 1674 (C=O), 1553 (C=C); ^1H NMR (DMSO- d_6) δ : 10.32 (brs, 1H, NH), 7.79–7.42 (m, 10H), 7.25 (d, J = 4.0 Hz, 2H), 7.15 (d, J = 4.0 Hz, 2H), 4.33 (s, 2H, SCH_2), 2.27, (s, 3H, OCH_3); ^{13}C NMR (DMSO- d_6) δ : 170.2, (C=O), 155.5, (triazole C-5), 149.6, (triazole C-3), 145.3, (*N*-phenyl C-1), 137.2, (*N*-phenyl C-1), 134.4, (phenyl C-4), 134.3, (naphthyl-C-4a), 131.1, (phenyl C-4), 129.2, (phenyl C-3, C-5), 128.6, (*N*-phenyl C-3, C-5), 128.3, (*N*-phenyl C-6), 127.6, (naphthyl C-3), 127.4, (phenyl C-2, C-6), 126.6, (*N*-phenyl C-2, C-6), 126.1, (naphthyl C-7), 125.7, (naphthyl C-8), 124.6, (naphthyl C-8a), 121.9, (naphthyl C-4), 107.2, (naphthyl C-2), 40.8, (SCH_2), 22.3 (CH_3); MS (m/z , %): 450 (M^+ , 8.09%). Anal. Calc. for $\text{C}_{27}\text{H}_{22}\text{N}_4\text{OS}$

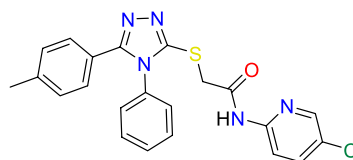
(M.W. = 450): C, 71.98; H, 4.92; N, 12.44; Found: C, 72.05; H, 5.00; N, 12.46%.

2-((4-Phenyl-5-(*p*-tolyl)-4*H*-1,2,4-triazol-3-yl)



thio)-N-(pyridin-2-yl)acetamide (17) White solid (0.28 g, 71%); mp = 238–240 °C; IR (KBr) ν_{\max} cm^{-1} : 3420 (NH), 3026 (CH aromatic), 2856 (CH aliphatic), 1667 (C=O), 1533 (C=C); ^1H NMR (DMSO- d_6) δ : 10.49 (brs, 1H, NH), 7.58 (d, J = 8.2 Hz, 2H), 7.54 (d, J = 9.6 Hz, 1H), 7.51 (d, J = 9.6 Hz, 1H), 7.42 (t, J = 8.2 Hz, 1H), 7.28 (t, J = 8.2 Hz, 1H), 7.23 (t, J = 8.2 Hz, 2H), 7.21 (d, J = 7.2 Hz, 2H), 7.15 (d, J = 7.4 Hz, 2H), 7.10 (t, J = 7.4, 1H), 4.18 (s, 2H, SCH_2), 2.29 (s, 3H, CH_3); ^{13}C NMR (DMSO- d_6) δ : 168.8, (C=O), 144.8, (triazole C-5), 139.3, (Pyridyl C-2), 138.9, (triazole C-3), 134.8, (Pyridyl C-6), 134.8, (*N*-phenyl C-1), 134.4, (Pyridyl C-4), 132.3, (phenyl C-1), 129.5, (phenyl C-4), 129.0, (phenyl C-3, C-5), 127.5, (*N*-phenyl C-3, C-5), 124.0, (*N*-phenyl C-4), 123.6, (*N*-phenyl C-2, C-6), 120.5, (phenyl C-2, C-6), 120.2, (Pyridyl C-5), 117.5, (Pyridyl C-3), 37.5, (SCH_2), 20.8, (CH_3); Anal. Calc. for $\text{C}_{22}\text{H}_{19}\text{N}_5\text{OS}$ (M.W. = 401): C, 65.82; H, 4.77; N, 17.44; Found: C, 65.93; H, 4.80; N, 17.48%.

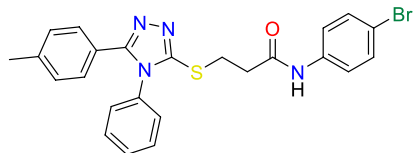
***N*-(5-Chloropyridin-2-yl)-2-((4-phenyl-5-(*p*-tolyl)-4*H*-1,2,4-**



-triazol-3-yl)thio)acetamide (18) White solid (0.32 g, 74%); mp = 239–241 °C; IR (KBr) ν_{\max} cm^{-1} : 3419 (NH), 3029 (CH aromatic), 2886 (CH aliphatic), 1666 (C=O), 1531 (C=C); ^1H NMR (DMSO- d_6) δ : 10.38 (brs, 1H, NH), 7.56 (d, J = 2.1 Hz, 2H), 7.54 (d, J = 3.9 Hz, 1H), 7.48 (d, J = 8.4, 1H), 7.44 (t, J = 3.3, 1H), 7.42 (t, J = 3.3 Hz, 2H), 7.40 (d, J = 4.5 Hz, 2H), 7.36 (d, J = 3.9 Hz, 2H), 7.12 (t, J = 8.1, 1H), 4.18 (s, 2H, SCH_2), 2.24 (s, 3H, CH_3); ^{13}C NMR (DMSO- d_6) δ : 168.7, (C=O), 144.8, (triazole C-5), 139.3, (Pyridyl C-2), 138.9, (triazole C-3), 134.8, (Pyridyl C-6), 134.8, (*N*-phenyl C-1), 134.4, (Pyridyl C-4), 132.4, (phenyl C-1), 129.6, (phenyl C-4), 129.0, (phenyl C-3, C-5), 127.5, (*N*-phenyl C-3, C-5), 124.0, (*N*-phenyl C-4), 123.7, (*N*-phenyl C-2, C-6), 120.4, (phenyl C-2, C-6), 120.1, (Pyridyl C-5), 117.6, (Pyridyl C-3), 37.6, (SCH_2), 21.0, (CH_3);

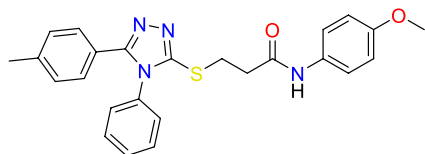
MS (m/z , %): 435 (M+, 1.17%), 437 (M+2, 0.47%). Anal. Calc. for $C_{22}H_{18}ClN_5OS$ (M.W. = 435): C, 60.62; H, 4.16; N, 16.07; Found: C, 60.64; H, 4.19; N, 16.12%.

***N*-(4-Bromophenyl)-3-((4-phenyl-5-(*p*-tolyl)-4*H*-1,2,4-tria-**



zol-3-yl)thio)propanamide (19) White solid (0.34 g, 69%); mp = 242–244 °C; IR (KBr) ν_{\max} cm^{-1} : 3424 (NH), 3042 (CH aromatic), 2935 (CH aliphatic), 1693 (C=O), 1537 (C=C); ^1H NMR (DMSO- d_6) δ : 10.11 (brs, 1H, NH), 7.52 (d, $J=2.4$ Hz, 2H), 7.23–6.84 (m, 11H), 3.41 (t, $J=6.3$, 2H, SCH_2), 2.84 (t, $J=6.6$, 2H, CH_2CO), 2.27 (s, 3H, CH_3); ^{13}C NMR (DMSO- d_6) δ : 169.5, (C=O), 154.3, (triazole C-5), 151.0, (triazole C-3), 144.2, (*N*-phenyl C-1), 139.4, (*NH*-phenyl C-1), 133.8, (phenyl C-4), 132.7, (phenyl C-1), 130.0, (*NH*-phenyl C-3, C-5), 129.9, (phenyl C-3, C-5), 129.3, (*N*-phenyl C-3, C-5), 129.1, (*N*-phenyl C-4), 128.5, (*N*-phenyl C-2, C-6), 127.7, (*NH*-phenyl C-2, C-6), 127.5, (*NH*-phenyl C-4), 123.7, (phenyl C-2, C-6), 36.8, (SCH_2), 20.8, (CH_3); MS (m/z , %): 493 (M+, 3.12%), 495 (M+2, 2.91%). Anal. Calc. for $C_{24}H_{21}BrN_4OS$ (M.W. = 493): C, 58.42; H, 4.29; N, 11.35; Found: C, 58.44; H, 4.32; N, 11.39%.

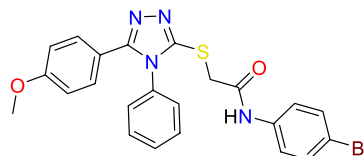
***N*-(4-Methoxyphenyl)-3-((4-phenyl-5-(*p*-tolyl)-4*H*-1,2,4-tria-**



zol-3-yl)thio)propanamide (20) White solid (0.29 g, 66%); mp = 226–228 °C; IR (KBr) ν_{\max} cm^{-1} : 3431 (NH), 3059 (CH aromatic), 2945 (CH aliphatic), 1680 (C=O), 1515 (C=C); ^1H NMR (DMSO- d_6) δ : 9.83 (brs, 1H, NH), 7.52 (d, $J=8.1$ Hz, 2H), 7.22 (d, $J=8.1$ Hz, 2H), 7.14 (d, $J=8.1$ Hz, 2H), 7.10–6.84 (m, 7H), 3.39 (t, $J=6.9$, 2H, SCH_2), 2.79 (t, $J=6.9$, 2H, CH_2CO), 3.71 (s, 3H, OCH_3); ^{13}C NMR (DMSO- d_6) δ : 169.4, (C=O), 154.2, (triazole C-5), 151.0, (triazole C-3), 144.1, (*N*-phenyl C-1), 139.3, (*NH*-phenyl C-1), 133.7, (phenyl C-4), 132.7, (phenyl C-1), 130.1, (*NH*-phenyl C-3, C-5), 129.8, (phenyl C-3, C-5), 129.3, (*N*-phenyl C-3, C-5), 129.0, (*N*-phenyl C-4), 128.4, (*N*-phenyl C-2, C-6), 127.7, (*NH*-phenyl C-2, C-6), 127.4, (*NH*-phenyl C-4),

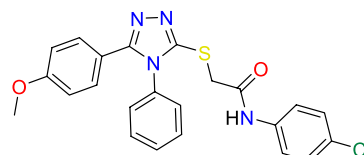
123.6, (phenyl C-2, C-6), 56.8 (OCH_3), 33.3, (CH_2CO), 29.4, (SCH_2), 21.3, (CH_3); MS (m/z , %): 493 (M+, 3.12%). Anal. Calc. for $C_{25}H_{24}N_4O_2S$ (M.W. = 444): C, 67.55; H, 5.44; N, 12.60; Found: C, 67.63; H, 5.48; N, 12.64%.

***N*-(4-Bromophenyl)-2-((5-(4-methoxyphenyl)-4-phenyl-4*H*-**



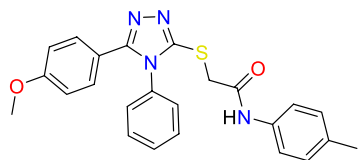
1,2,4-triazol-3-yl)thio)acetamide (21) White solid (0.36 g, 74%); mp = 243–245 °C; ^1H NMR (DMSO- d_6) δ : 10.56 (brs, 1H, NH), 7.56–7.48 (m, 5H), 7.41 (d, $J=8.4$ Hz, 2H), 7.36 (d, $J=8.8$ Hz, 2H), 7.28 (d, $J=8.0$ Hz, 2H), 6.90 (d, $J=8.4$ Hz, 2H), 4.16 (s, 2H, SCH_2), 3.72 (s, 3H, OCH_3); ^{13}C NMR (DMSO- d_6) δ : 164.9, (C=O), 155.3, (triazole C-5), 151.6, (triazole C-3), 133.7, (*N*-phenyl C-1), 131.9, (*NH*-phenyl C-1), 130.0, (phenyl C-3, C-5), 129.9, (*N*-phenyl C-3, C-5), 128.5, (phenyl C-1, C-4), 127.8, (*N*-phenyl C-2, C-6), 127.6, (*NH*-phenyl C-2, C-6), 126.5, (*N*-phenyl C-4), 120.6, (phenyl C-2, C-6), 113.9, (*NH*-phenyl C-4), 55.1, (OCH_3), 36.8, (SCH_2); MS (m/z , %): 494 (M+, 0.8%). Anal. Calc. for $C_{23}H_{19}BrN_4O_2S$ (M.W. = 494): C, 55.76; H, 3.87; N, 11.31; Found: C, 55.88; H, 3.89; N, 11.36%.

***N*-(4-Chlorophenyl)-2-((5-(4-methoxyphenyl)-4-phenyl-4*H*-1,2,**

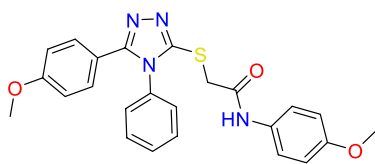


4-triazol-3-yl)thio)acetamide (22) White solid (0.36 g, 80%); mp = 239–241 °C; ^1H NMR (DMSO- d_6) δ : 10.50 (brs, 1H, NH), 7.61–7.54 (m, 5H), 7.42 (d, $J=8.4$ Hz, 2H), 7.38 (d, $J=8.8$ Hz, 2H), 7.28 (d, $J=8.8$ Hz, 2H), 6.90 (d, $J=8.8$ Hz, 2H), 4.16 (s, 2H, SCH_2), 3.72 (s, 3H, OCH_3); ^{13}C NMR (DMSO- d_6) δ : 165.6, (C=O), 153.4, (triazole C-5), 161.0, (phenyl C-4), 151.8, (triazole C-3), 137.7, (*N*-phenyl C-1), 134.6, (*NH*-phenyl C-1), 133.4, (phenyl C-3, C-5), 130.2, (*N*-phenyl C-3, C-5), 130.0, (*N*-phenyl C-4 & phenyl C-1), 129.6, (*N*-phenyl C-2, C-6), 128.7, (*NH*-phenyl C-2, C-6), 127.5, (*N*-phenyl C-4), 127.0, (phenyl C-2, C-6), 125.3, (*NH*-phenyl C-4), 56.1, (OCH_3), 36.7, (SCH_2); MS (m/z , %): 452 (M+2, 0.98%), 452 (M+, 157%). Anal. Calc. for $C_{23}H_{19}ClN_4O_2S$ (M.W. = 450): C, 61.26; H, 4.25; N, 12.42; Found: C, 61.29; H, 4.27; N, 12.48%.

2-((5-(4-Methoxyphenyl)-4-phenyl-4H-1,2,4-triazol-3-yl)

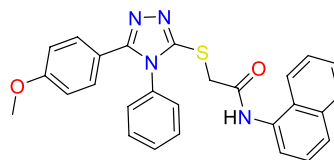


thio-N-(p-tolyl)acetamide (23) White solid (0.30 g, 70%); mp = 219–221 °C; IR (KBr) ν_{\max} cm^{-1} : 3431 (NH), 3081 (CH aromatic), 2964 (CH aliphatic), 1680 (C=O), 1523 (C=C); $^1\text{H NMR}$ (DMSO- d_6) δ : 10.26 (brs, 1H, NH), 7.55–7.42 (m, 7H), 7.29 (d, $J=8.0$ Hz, 2H), 7.12 (d, $J=7.6$ Hz, 2H), 6.90 (d, $J=8.0$ Hz, 2H), 4.16 (s, 2H, SCH_2), 3.72 (s, 3H, OCH_3), 2.24 (s, 3H, CH_3); $^{13}\text{C NMR}$ (DMSO- d_6) δ : 165.6, (C=O), 153.5, (triazole C-5), 151.8, (phenyl C-1), 137.7, (triazole C-3), 134.6, (*N*-phenyl C-1), 133.5, (NH-phenyl C-1), 130.3, (phenyl C-3, C-5), 130.1, (*N*-phenyl C-3, C-5), 129.6, (phenyl C-4), 128.8, (*N*-phenyl C-2, C-6), 127.6, (NH-phenyl C-2, C-6), 127.0, (*N*-phenyl C-4), 125.3, (phenyl C-2, C-6), 120.6, (NH-phenyl C-4), 56.3, (OCH_3), 36.7, (SCH_2), 20.6, (CH_3); MS (m/z , %): 430 (M^+ , 10.81%). Anal. Calc. for $\text{C}_{24}\text{H}_{22}\text{N}_4\text{O}_2\text{S}$ (M.W. = 430): C, 66.96; H, 5.15; N, 13.01; Found: C, 67.06; H, 5.18; N, 13.07%.

N-(4-Methoxyphenyl)-2-((5-(4-methoxyphenyl)-4-phenyl-4H

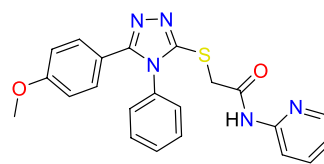
-1,2,4-triazol-3-yl)thio)acetamide (24) White solid (0.28 g, 65%); mp = 226–228 °C; IR (KBr) ν_{\max} cm^{-1} : 3460 (NH), 3073 (CH aromatic), 2952 (CH aliphatic), 1681 (C=O), 1542 (C=C); $^1\text{H NMR}$ (DMSO- d_6) δ : 10.21 (brs, 1H, NH), 7.56–7.42 (m, 7H), 7.28 (d, $J=8.0$ Hz, 2H), 6.90 (d, $J=8.4$ Hz, 4H), 4.13 (s, 2H, SCH_2), 3.72 (s, 3H, OCH_3), 3.71 (s, 3H, OCH_3); $^{13}\text{C NMR}$ (DMSO- d_6) δ : 169.8, (C=O), 158.8, (phenyl C-4), 144.8, (NH-phenyl C-4), 139.3, (triazole C-5), 138.9, (triazole C-3), 136.0, (*N*-phenyl C-1), 134.3, (NH-phenyl C-1), 132.2, (phenyl C-3, C-5), 130.1, (*N*-phenyl C-3, C-5), 128.9, (phenyl C-4), 127.5, (*N*-phenyl C-2, C-6), 123.9, (NH-phenyl C-2, C-6), 123.5, (*N*-phenyl C-4), 120.5, (phenyl C-2, C-6), 117.5, (NH-phenyl C-4), 55.4, (OCH_3), 55.1, (OCH_3), 37.1, (SCH_2); MS (m/z , %): 446 (M^+ , 1.60%). Anal. Calc. for $\text{C}_{24}\text{H}_{22}\text{N}_4\text{O}_3\text{S}$ (M.W. = 446): C, 64.56; H, 4.97; N, 12.55; Found: C, 64.60; H, 5.01; N, 12.59%.

2-((5-(4-Methoxyphenyl)-4-phenyl-4H-1,2,4-triazol-3-yl)

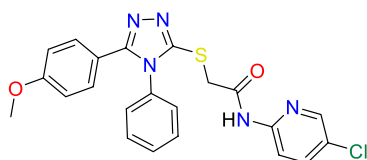


thio-N-(naphthalen-1-yl)acetamide (25) White solid (0.32 g, 70%); mp = 227–229 °C; $^1\text{H NMR}$ (DMSO- d_6) δ : 10.34 (brs, 1H, NH), 7.56–7.49 (m, 8H), 7.42 (d, $J=8.4$ Hz, 4H), 7.28 (d, $J=8.8$ Hz, 2H), 6.90 (d, $J=9.2$ Hz, 2H), 4.17 (s, 2H, SCH_2), 3.82, (s, 3H, OCH_3); $^{13}\text{C NMR}$ (DMSO- d_6) δ : 167.1, (C=O), 158.3, (phenyl C-4), 144.8, (triazole C-5), 142.3, (triazole C-3), 139.3, (*N*-phenyl C-1), 138.8, (*N*-phenyl C-1), 134.1, (naphthyl C-4a), 132.2, (phenyl C-4), 130.0, (phenyl C-3, C-5), 129.3, (*N*-phenyl C-3, C-5), 128.3, (*N*-phenyl C-6), 127.5, (naphthyl C-3), 124.1, (phenyl C-2, C-6), 123.6, (*N*-phenyl C-2, C-6), 120.5, (naphthyl C-7), 120.3, (naphthyl C-8), 118.5, (naphthyl C-8a), 117.6, (naphthyl C-4), 114.5, (naphthyl C-2), 56.1, (OCH_3), 42.3, (SCH_2); MS (m/z , %): 466 (M^+ , 8.09%). Anal. Calc. for $\text{C}_{27}\text{H}_{22}\text{N}_4\text{O}_2\text{S}$ (M.W. = 466): C, 69.51; H, 4.75; N, 12.01; Found: C, 69.58; H, 4.77; N, 12.10%.

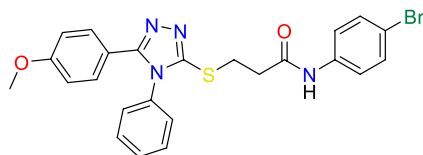
2-((5-(4-Methoxyphenyl)-4-phenyl-4H-1,2,4-triazol-3-yl)



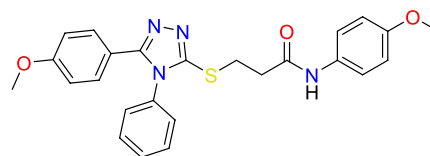
thio-N-(pyridin-2-yl)acetamide (26) White solid (0.29 g, 70%); mp = 252–254 °C; IR (KBr) ν_{\max} cm^{-1} : 3428 (NH), 3027 (CH aromatic), 2872 (CH aliphatic), 1665 (C=O), 1536 (C=C); $^1\text{H NMR}$ (DMSO- d_6) δ : 10.49 (brs, 1H, NH), 7.58 (d, $J=8.8$ Hz, 2H), 7.53 (d, $J=7.6$ Hz, 1H), 7.51 (d, $J=7.2$ Hz, 1H), 7.42 (t, $J=7.2$ Hz, 1H), 7.28 (t, $J=7.2$ Hz, 1H), 7.23 (t, $J=7.2$ Hz, 2H), 7.21 (d, $J=7.2$ Hz, 2H), 7.15 (d, $J=7.6$ Hz, 2H), 7.11 (t, $J=9.2$ Hz, 1H), 4.20 (s, 2H, SCH_2), 3.72 (s, 3H, OCH_3); $^{13}\text{C NMR}$ (DMSO- d_6) δ : 168.8, (C=O), 144.8, (triazole C-5), 139.2, (Pyridyl C-2), 138.9, (triazole C-3), 134.9, (Pyridyl C-6), 134.8, (*N*-phenyl C-1), 134.4, (Pyridyl C-4), 132.1, (phenyl C-1), 129.6, (phenyl C-4), 129.2, (phenyl C-3, C-5), 127.6, (*N*-phenyl C-3, C-5), 124.4, (*N*-phenyl C-4), 123.0, (*N*-phenyl C-2, C-6), 120.5, (phenyl C-2, C-6), 120.2, (Pyridyl C-5), 117.4, (Pyridyl C-3), 55.7, (OCH_3), 37.7, (SCH_2); Anal. Calc. for $\text{C}_{22}\text{H}_{19}\text{N}_5\text{O}_2\text{S}$ (M.W. = 417): C, 63.29; H, 4.59; N, 16.78; Found: C, 63.38; H, 4.61; N, 16.80%.

***N*-(5-Chloropyridin-2-yl)-2-((5-(4-methoxyphenyl)-4-phenyl-4H-1,2,4-triazol-3-yl)thio)acetamide**

(27) White solid (0.34 g, 75%); mp = 242–244 °C; IR (KBr) ν_{\max} cm^{-1} : 3423 (NH), 3071 (CH aromatic), 2968 (CH aliphatic), 1673 (C=O); ^1H NMR (DMSO- d_6) δ : 10.19 (brs, 1H, NH), 7.58 (d, $J=4.2$ Hz, 2H), 7.56 (d, $J=3.6$ Hz, 1H), 7.54 (d, $J=3.6$ Hz, 1H), 7.46 (t, $J=6.3$ Hz, 1H), 7.43 (t, $J=3.0$ Hz, 2H), 7.40 (d, $J=3.6$ Hz, 2H), 7.34 (d, $J=1.9$ Hz, 2H), 6.90 (t, $J=9.0$ Hz, 1H), 4.16 (s, 2H, SCH_2), 3.72 (s, 3H, OCH_3); ^{13}C NMR (DMSO- d_6) δ : 168.6, (C=O), 144.8, (triazole C-5), 139.3, (Pyridyl C-2), 138.9, (triazole C-3), 134.8, (Pyridyl C-6), 134.8, (*N*-phenyl C-1), 134.4, (Pyridyl C-4), 132.4, (phenyl C-1), 129.6, (phenyl C-4), 129.1, (phenyl C-3, C-5), 127.4, (*N*-phenyl C-3, C-5), 124.0, (*N*-phenyl C-4), 123.8, (*N*-phenyl C-2, C-6), 120.5, (phenyl C-2, C-6), 120.1, (Pyridyl C-5), 117.3, (Pyridyl C-3), 58.7, (OCH_3), 37.8, (SCH_2). Anal. Calc. for $\text{C}_{22}\text{H}_{18}\text{ClN}_5\text{O}_2\text{S}$ (M.W. = 435): C, 58.47; H, 4.01; N, 15.50; Found: C, 58.51; H, 4.04; N, 15.57%.

***N*-(4-Bromophenyl)-3-((5-(4-methoxyphenyl)-4-phenyl-4H-1,**

2,4-triazol-3-yl)thio)propanamide (28) White solid (0.34 g, 67%); mp = 246–248 °C; IR (KBr) ν_{\max} cm^{-1} : 3426 (NH), 3062 (CH aromatic), 2920 (CH aliphatic), 1676 (C=O), 1542 (C=C); ^1H NMR (DMSO- d_6) δ : 10.11 (brs, 1H, NH), 7.55–7.35 (m, 9H), 7.27 (d, $J=2.1$ Hz, 2H), 6.90 (d, $J=8.7$ Hz, 2H), 3.73 (s, 3H, OCH_3), 3.37 (t, $J=6.9$ Hz, 2H, SCH_2), 2.84 (s, 2H, CH_2CO); ^{13}C NMR (DMSO- d_6) δ : 169.5, (C=O), 154.32, (triazole C-5), 151.0, (triazole C-3), 144.2, (*N*-phenyl C-1), 139.4, (*NH*-phenyl C-1), 133.8, (phenyl C-4), 132.7, (phenyl C-1), 130.0, (*NH*-phenyl C-3, C-5), 129.9, (phenyl C-3, C-5), 129.3, (*N*-phenyl C-3, C-5), 129.1, (*N*-phenyl C-4), 128.5, (*N*-phenyl C-2, C-6), 127.7, (*NH*-phenyl C-2, C-6), 127.5, (*NH*-phenyl C-4), 123.6, (phenyl C-2, C-6), 56.1, (OCH_3), 33.2, (SCH_2), 29.4, (CH_2); MS (m/z , %): 509 (M+, 2.83%), 511 (M+2, 2.62%). Anal. Calc. for $\text{C}_{24}\text{H}_{21}\text{BrN}_4\text{O}_2\text{S}$ (M.W. = 509): C, 56.59; H, 4.16; N, 11.00; Found: C, 56.71; H, 4.22; N, 11.09%.

***N*-(4-Methoxyphenyl)-3-((5-(4-methoxyphenyl)-4-phenyl-**

4H-1,2,4-triazol-3-yl)thio)propanamide (29) White solid (0.27 g, 60%); mp = 227–229 °C; IR (KBr) ν_{\max} cm^{-1} : 3431 (NH), 3059 (CH aromatic), 2945 (CH aliphatic), 1680 (C=O), 1515 (C=C); ^1H NMR (DMSO- d_6) δ : 9.83 (brs, 1H, NH), 7.39–7.52 (m, 9H), 7.28 (d, $J=6.9$ Hz, 2H), 6.90 (d, $J=9.0$ Hz, 2H), 3.72 (s, 3H, OCH_3), 3.70 (s, 3H, OCH_3), 3.71 (t, $J=6.9$ Hz, 2H, SCH_2), 2.79 (t, $J=6.9$ Hz, 2H, CH_2CO); ^{13}C NMR (DMSO- d_6) δ : 170.0, (C=O), 154.3, (triazole C-5), 151.1, (triazole C-3), 144.2, (*N*-phenyl C-1), 139.5, (*NH*-phenyl C-1), 133.8, (phenyl C-4), 132.8, (phenyl C-1), 130.1, (*NH*-phenyl C-3, C-5), 129.8, (phenyl C-3, C-5), 129.1, (*N*-phenyl C-3, C-5), 129.0, (*N*-phenyl C-4), 128.3, (*N*-phenyl C-2, C-6), 127.6, (*NH*-phenyl C-2, C-6), 127.5, (*NH*-phenyl C-4), 123.6, (phenyl C-2, C-6), 56.2, (2OCH_3), 33.1, (SCH_2), 29.4, (CH_2); MS (m/z , %): 460 (M+, 1.39%). Anal. Calc. for $\text{C}_{25}\text{H}_{24}\text{N}_4\text{O}_3\text{S}$ (M.W. = 460): C, 65.20; H, 5.25; N, 12.17; Found: C, 65.27; H, 5.28; N, 12.24%.

Biological evaluation**In vitro cytotoxic activity**

The antitumor activity of new triazoles against MDA-MB-231 cells was evaluated by using the tetrazolium salt 3-(4,5-dimethyl-2-thiazolyl)-2,5-diphenyl-2H-tetrazolium bromide (MTT) assay in accordance with a reported method [50].

In silico cytotoxicity and ADMET profiles

In silico CLC-prediction system [43] and pkCSM descriptors algorithm protocol [47] were used to predict the cytotoxicity and to study ADMET profiles of new triazoles.

Docking studies

In the present study, all docking experiments were performed for all the final target hybrid structures using Molecular Operating Environment software (MOE2014, <https://www.chemcomp.com/Products.htm>) to evaluate the binding free energy and to explore the binding mode toward STAT3

(PDB: 6NJS, Resolution: 2.70 Å, <https://www.rcsb.org/structure/6NJS>) and considered as a target for docking simulation [45]. Firstly, the crystal structure of the protein was prepared by removing water molecules and retaining the essential chain and the co-crystallized ligand. After that, protein protonated, the energy minimized, and the binding pocket of the protein defined. The 3D structures of new triazoles were sketched using Chem3D 15.0, energy minimized, and finally saved in molfile format. Molecular docking of final target compounds was performed by the default protocol against the target receptor. In each case, 10 docked poses were generated using genetic algorithm searches, and Affinity dG & London dG were used for scoring 1 and Scoring 2, respectively. The London dG scoring function predicts the free energy of binding of the ligand from a given pose. The functional form is a sum of terms:

$$\Delta G = C + E_{\text{flex}} + \sum_{\text{h-bond}} C_{\text{HB}} F_{\text{HB}} + \sum_{\text{m-lig}} C_{\text{M}} F_{\text{M}} + \sum_{\text{atom } i} \Delta D_i$$

where C is the average gain or loss of rotational and translational entropy; E_{flex} represents the energy upon loss of flexibility of the ligand; C_{HB} and F_{HB} are the energy of an ideal hydrogen bond and the geometric imperfections of hydrogen bonds, respectively; C_{M} and F_{M} represent the energy of an ideal metal ligation and the measure of geometric imperfections of metal ligations, respectively; D_i is the dissolution energy of an atom i .

Compliance with ethical standards

Conflict of interest The authors declare that they have no conflict of interest.

References

- Jiang DM, Chan KKW, Jang RW et al (2019) Anticancer drugs approved by the Food and Drug Administration for gastrointestinal malignancies: clinical benefit and price considerations. *Cancer Med* 8:1584–1593. <https://doi.org/10.1002/cam4.2058>
- Wu Q, Yang Z, Nie Y et al (2014) Multi-drug resistance in cancer chemotherapeutics: mechanisms and lab approaches. *Cancer Lett* 347:159–166. <https://doi.org/10.1016/j.canlet.2014.03.013>
- Ihle JN (2001) The Stat family in cytokine signaling. *Curr Opin Cell Biol* 13:211–217. [https://doi.org/10.1016/S0955-0674\(00\)00199-X](https://doi.org/10.1016/S0955-0674(00)00199-X)
- Ghosh S (2019) Cisplatin: the first metal based anticancer drug. *Bioorg Chem* 88:102925. <https://doi.org/10.1016/j.bioorg.2019.102925>
- Heidelberger S, Zinzalla G, Antonow D et al (2013) Investigation of the protein alkylation sites of the STAT3:STAT3 inhibitor Statibic by mass spectrometry. *Bioorg Med Chem Lett* 23:4719–4722. <https://doi.org/10.1016/j.bmcl.2013.05.066>
- Hong DS, Angelo LS, Kurzrock R (2007) Interleukin-6 and its receptor in cancer. *Cancer* 110:1911–1928. <https://doi.org/10.1002/cncr.22999>
- Lee H, Deng J, Kujawski M et al (2010) STAT3-induced S1PR1 expression is crucial for persistent STAT3 activation in tumors. *Nat Med* 16:1421–1428. <https://doi.org/10.1038/nm.2250>
- Sgrignani J, Garofalo M, Matkovic M et al (2018) Structural biology of STAT3 and its implications for anticancer therapies development. *Int J Mol Sci* 19:1591. <https://doi.org/10.3390/ijms19061591>
- Chen H, Guan Y, Yuan G et al (2014) A perylene derivative regulates HIF-1 α and Stat3 signaling pathways. *Bioorg Med Chem* 22:1496–1505. <https://doi.org/10.1016/j.bmc.2013.10.018>
- Robinson AJ, Kunji ERS, Gross A (2012) Mitochondrial carrier homolog 2 (MTCH2): the recruitment and evolution of a mitochondrial carrier protein to a critical player in apoptosis. *Exp Cell Res* 318:1316–1323. <https://doi.org/10.1016/j.yexcr.2012.01.026>
- Lee JH, Kim JE, Kim BG et al (2016) STAT3-induced WDR1 overexpression promotes breast cancer cell migration. *Cell Signal* 28:1753–1760. <https://doi.org/10.1016/j.cellsig.2016.08.006>
- Sánchez-Ceja SG, Reyes-Maldonado E, Vázquez-Manríquez ME et al (2006) Differential expression of STAT5 and Bcl-xL, and high expression of Neu and STAT3 in non-small-cell lung carcinoma. *Lung Cancer* 54:163–168. <https://doi.org/10.1016/j.lungcan.2006.07.012>
- Ke Y, Bao T, Wu X et al (2017) Scutellarin suppresses migration and invasion of human hepatocellular carcinoma by inhibiting the STAT3/Girdin/Akt activity. *Biochem Biophys Res Commun* 483:509–515. <https://doi.org/10.1016/j.bbrc.2016.12.114>
- Mahanti S, Sunkara S, Bhavani R (2019) Synthesis, biological evaluation and computational studies of fused acridine containing 1,2,4-triazole derivatives as anticancer agents. *Synth Commun* 49:1729–1740. <https://doi.org/10.1080/00397911.2019.1608450>
- Mioc M, Avram S, Bercean V et al (2018) Design, synthesis and biological activity evaluation of S-substituted 1H-5-Mercapto-1,2,4-triazole derivatives as antiproliferative agents in colorectal cancer. *Front Chem*. <https://doi.org/10.3389/fchem.2018.00373>
- Ghanaat J, Khalilzadeh MA, Zareyee D (2020) Molecular docking studies, biological evaluation and synthesis of novel 3-mercapto-1,2,4-triazole derivatives. *Mol Divers*. <https://doi.org/10.1007/s11030-020-10050-0>
- Tariq S, Kamboj P, Alam O, Amir M (2018) 1,2,4-Triazole-based benzothiazole/benzoxazole derivatives: design, synthesis, p38 α MAP kinase inhibition, anti-inflammatory activity and molecular docking studies. *Bioorg Chem* 81:630–641. <https://doi.org/10.1016/j.bioorg.2018.09.015>
- Bejot R, Kersemans V, Kelly C et al (2010) Pre-clinical evaluation of a 3-nitro-1,2,4-triazole analogue of [18F]FMISO as hypoxia-selective tracer for PET. *Nucl Med Biol* 37:565–575. <https://doi.org/10.1016/j.nucmedbio.2010.03.011>
- Boraei ATA, Singh PK, Sechi M, Satta S (2019) Discovery of novel functionalized 1,2,4-triazoles as PARP-1 inhibitors in breast cancer: design, synthesis and antitumor activity evaluation. *Eur J Med Chem* 182:111621. <https://doi.org/10.1016/j.ejmech.2019.111621>
- Kulabaş N, Tatar E, Bingöl Özakpınar Ö et al (2016) Synthesis and antiproliferative evaluation of novel 2-(4H-1,2,4-triazole-3-ylthio)acetamide derivatives as inducers of apoptosis in cancer cells. *Eur J Med Chem* 121:58–70. <https://doi.org/10.1016/j.ejmech.2016.05.017>
- Ali AR, El-Bendary ER, Ghaly MA, Shehata IA (2013) Novel acetamidothiazole derivatives: synthesis and in vitro anti-cancer evaluation. *Eur J Med Chem* 69:908–919. <https://doi.org/10.1016/j.ejmech.2013.08.021>

22. Ezzat HG, Bayoumi AH, Sherbiny FF et al (2020) Design, synthesis, and molecular docking studies of new [1,2,4]triazolo[4,3-a]quinoxaline derivatives as potential A2B receptor antagonists. *Mol Divers*. <https://doi.org/10.1007/s11030-020-10070-w>
23. El-Morsy AM, El-Sayed MS, Abulkhair HS (2017) Synthesis, characterization and in vitro antitumor evaluation of new pyrazolo[3,4-d]pyrimidine derivatives. *Open J Med Chem* 07:1–17. <https://doi.org/10.4236/ojmc.2017.71001>
24. Lu X, Li X, Yang J et al (2016) Arylazolyl(aziny)thioacetanilides. Part 20: discovery of novel purinylthioacetanilides derivatives as potent HIV-1 NNRTIs via a structure-based bioisosterism approach. *Bioorg Med Chem* 24:4424–4433. <https://doi.org/10.1016/j.bmc.2016.07.041>
25. El-Helby A-GA, Sakr H, Eissa IH et al (2019) Design, synthesis, molecular docking, and anticancer activity of benzoxazole derivatives as VEGFR-2 inhibitors. *Arch Pharm (Weinheim)*. <https://doi.org/10.1002/ardp.201900113>
26. Matsuno K, Masuda Y, Uehara Y et al (2010) Identification of a new series of STAT3 inhibitors by virtual screening. *ACS Med Chem Lett* 1:371–375. <https://doi.org/10.1021/ml1000273>
27. Kaoud TS, Mohassab AM, Hassan HA et al (2020) NO-releasing STAT3 inhibitors suppress BRAF-mutant melanoma growth. *Eur J Med Chem* 186:111885. <https://doi.org/10.1016/j.ejmech.2019.111885>
28. Han J, Lim W, You D et al (2019) Chemoresistance in the human triple-negative breast cancer cell line MDA-MB-231 induced by doxorubicin gradient is associated with epigenetic alterations in histone deacetylase. *J Oncol* 2019:1–12. <https://doi.org/10.1155/2019/1345026>
29. Theodosiou TA, Ali M, Grigalavicius M et al (2019) Simultaneous defeat of MCF7 and MDA-MB-231 resistances by a hypericin PDT-tamoxifen hybrid therapy. *NPJ Breast Cancer* 5:13. <https://doi.org/10.1038/s41523-019-0108-8>
30. Ali A, Bhattacharya S (2014) DNA binders in clinical trials and chemotherapy. *Bioorg Med Chem* 22:4506–4521. <https://doi.org/10.1016/j.bmc.2014.05.030>
31. Abulkhair HS, Turki A, Ghiaty A et al (2020) Novel triazolophthalazine-hydrazone hybrids as potential PCAF inhibitors: design, synthesis, in vitro anticancer evaluation, apoptosis, and molecular docking studies. *Bioorg Chem*. <https://doi.org/10.1016/j.bioorg.2020.103899>
32. Turki A, Bayoumi AH, Ghiaty A et al (2020) Design, synthesis, and antitumor activity of novel compounds based on 1,2,4-triazolophthalazine scaffold: apoptosis-inductive and PCAF-inhibitory effects. *Bioorg Chem*. <https://doi.org/10.1016/j.bioorg.2020.104019>
33. Ihmaid S, Ahmed HEA, Al-Sheikh Ali A et al (2017) Rational design, synthesis, pharmacophore modeling, and docking studies for identification of novel potent DNA-PK inhibitors. *Bioorg Chem* 72:234–247. <https://doi.org/10.1016/j.bioorg.2017.04.014>
34. Oliveira Pedrosa M, Duarte da Cruz R, Oliveira Viana J et al (2017) hybrid compounds as direct multitarget ligands: a review. *Curr Top Med Chem* 17:1044–1079. <https://doi.org/10.2174/1568026616666160927160620>
35. Harrison JR, Brand S, Smith V et al (2018) A molecular hybridization approach for the design of potent, highly selective, and brain-penetrant N-myristoyltransferase inhibitors. *J Med Chem* 61:8374–8389. <https://doi.org/10.1021/acs.jmedchem.8b00884>
36. Bayoumi A, Ghiaty A, El-Morsy A et al (2012) Synthesis and evaluation of some new 1,2,4-triazolo(4,3-a)quinoxalin-4-5H-one derivatives as AMPA receptor antagonists. *Bull Fac Pharmacy, Cairo Univ* 50:141–146. <https://doi.org/10.1016/j.bfopu.2012.05.002>
37. Pagadala R, Meshram JS, Chopde HN et al (2012) Synthesis and antimicrobial evaluation of new monocyclic β -lactams. *J Heterocycl Chem* 49:1151–1155. <https://doi.org/10.1002/jhet.973>
38. Abul-Khair H, Elmeligie S, Bayoumi A et al (2013) Synthesis and evaluation of some new (1,2,4) Triazolo(4,3-a)Quinoxalin-4(5H)-one derivatives as AMPA receptor antagonists. *J Heterocycl Chem* 50:1202–1208. <https://doi.org/10.1002/jhet.714>
39. El-Helby AA, Ayyad RRA, Zayed MF et al (2019) Design, synthesis, in silico ADMET profile and GABA—a docking of novel phthalazines as potent anticonvulsants. *Arch Pharm (Weinheim)* 352:1800387. <https://doi.org/10.1002/ardp.201800387>
40. Eid I, Elsebaei MM, Mohammad H et al (2017) Arylthiazole antibiotics targeting intracellular methicillin-resistant *Staphylococcus aureus* (MRSA) that interfere with bacterial cell wall synthesis. *Eur J Med Chem* 139:665–673. <https://doi.org/10.1016/j.ejmech.2017.08.039>
41. Hannoun MH, Hagra M, Kotb A et al (2020) Synthesis and antibacterial evaluation of a novel library of 2-(thiazol-5-yl)-1,3,4-oxadiazole derivatives against methicillin-resistant *Staphylococcus aureus* (MRSA). *Bioorg Chem*. <https://doi.org/10.1016/j.bioorg.2019.103364>
42. Omar AM, Ihmaid S, Habib E-SE et al (2020) The rational design, synthesis, and antimicrobial investigation of 2-Amino-4-Methylthiazole analogues inhibitors of GlcN-6-P synthase. *Bioorg Chem*. <https://doi.org/10.1016/j.bioorg.2020.103781>
43. Lagunin AA, Dubovskaja VI, Rudik AV et al (2018) CLC-Pred: a freely available web-service for in silico prediction of human cell line cytotoxicity for drug-like compounds. *PLoS ONE* 13:e0191838. <https://doi.org/10.1371/journal.pone.0191838>
44. Morgan DML (ed) (1998) Tetrazolium (MTT) Assay for cellular viability and activity. In: Polyamine protocols. *Methods in molecular biology*TM, vol 79. Humana Press. <https://doi.org/10.1385/0-89603-448-8:179>
45. Bai L, Zhou H, Xu R et al (2019) A potent and selective small-molecule degrader of STAT3 achieves complete tumor regression in vivo. *Cancer Cell* 36:498–511.e17. <https://doi.org/10.1016/j.ccell.2019.10.002>
46. Lipinski CA, Lombardo F, Dominy BW, Feeney PJ (1997) Experimental and computational approaches to estimate solubility and permeability in drug discovery and development settings. *Adv Drug Deliv Rev* 23:3–25. [https://doi.org/10.1016/S0169-409X\(96\)00423-1](https://doi.org/10.1016/S0169-409X(96)00423-1)
47. DE Pires V, Blundell TL, Ascher DB (2015) pkCSM: predicting small-molecule pharmacokinetic and toxicity properties using graph-based signatures. *J Med Chem* 58:4066–4072. <https://doi.org/10.1021/acs.jmedchem.5b00104>
48. Beig A, Agbaria R, Dahan A (2013) Oral delivery of lipophilic drugs: the tradeoff between solubility increase and permeability decrease when using cyclodextrin-based formulations. *PLoS ONE* 8:e68237. <https://doi.org/10.1371/journal.pone.0068237>
49. Murty MSR, Ram KR, Venkateswara Rao R et al (2012) Synthesis of new S-alkylated-3-mercapto-1,2,4-triazole derivatives bearing cyclic amine moiety as potent anticancer agents. *Lett Drug Des Discov* 9:276–281. <https://doi.org/10.2174/157018012799129882>
50. Mosmann T (1983) Rapid colorimetric assay for cellular growth and survival: application to proliferation and cytotoxicity assays. *J Immunol Methods* 65:55–63

Publisher's Note Springer Nature remains neutral with regard to jurisdictional claims in published maps and institutional affiliations.